

2012/01/27  
2012  
2012/01/27

**MONITORING AND CHARACTERIZATION  
OF A BATCH REACTION – FOR ON-LINE  
RECIPE ADJUSTMENT**

By

**SYED SAMIR ALAM**

Bachelor of Science

Oklahoma State University

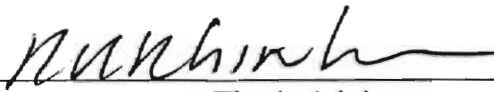
Stillwater, Oklahoma

2001

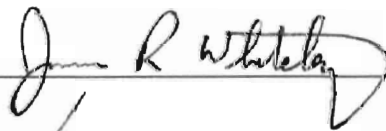
Submitted to the Faculty of the  
Graduate College of the  
Oklahoma State University  
In partial fulfillment of  
The requirements for the Degree of  
**MASTER OF SCIENCE**  
December 2003

**MONITORING AND CHARACTERIZATION  
OF A BATCH REACTION – FOR ON-LINE  
RECIPE ADJUSTMENT**

Thesis approved:



Thesis Advisor



Dean of Graduate College

## **Preface**

New techniques have been developed for experimental optimization of batch recipes in real-time. The novelty of the approach is to observe the batch progress online, to use in-situ spectroscopic measurements to adjust values of model coefficients of the reaction system on-line, and to use the up-dated model to determine an optimum recipe for the remainder of the batch process. The methodology is illustrated using experimental and simulated semi-batch reactor data.

## **Acknowledgements**

I would like to thank Dr. R. Russell Rhinehart, my advisor, for his guidance and advice. I have learnt a great deal from him and I greatly appreciate his expertise and knowledge and the fact that he was always available to help.

Special thanks to Dr. Paul J. Gemperline and Shane Stephen Moore and all the other students at the Department of Chemistry, Eastern Carolina University, Greenville, NC, who worked and helped with the experimental part of this project and provided me with quality data.

I appreciate, the financial support offered by the industrial sponsors of the Measurement and Control Engineering Center (MCEC), and the opportunity provided to me by the School of Chemical Engineering at Oklahoma State University to let me work on state of the art technology with such brilliant people.

I thank my committee members for their time and guidance. I would also like to thank my family and friends for their support.

## TABLE OF CONTENTS

Chapter	Page
<b>1. INTRODUCTION</b>	<b>1</b>
<b>2. BACKGROUND</b>	<b>4</b>
OFF-LINE OPTIMIZATION	4
ON-LINE OPTIMIZATION	5
Model Based Optimization	5
Model Free Optimization	8
CHEMICAL ANALYSIS TOOLS	8
Spectroscopy	9
END-POINT DETERMINATION:	10
<b>3. EXPERIMENTATION</b>	<b>11</b>
INTRODUCTION	11
REACTION MECHANISM	14
DATA ACQUISITION AND CONTROL	16
INSTRUMENTATION	18
Calorimeter System	18

UV/Vis Fiber-optic CCD spectrometer-----	20
Spectra Processing -----	23
REACTION CONDITIONS -----	25
<b>4. THE ALGORITHM-----</b>	<b>28</b>
ALGORITHM BASIS-----	28
ALGORITHM -----	29
Kinetic Model -----	29
<b>5. SIMULATIONS-----</b>	<b>38</b>
PROCESS SIMULATOR-----	38
<b>6. RESULTS AND DISCUSSION -----</b>	<b>40</b>
EXPERIMENTAL RESULTS -----	40
Experiment 1: 5_01_03 -----	40
Experiment 3 -----	43
Experiment 4 -----	45
Constant Ratio-----	46
Presence of Water-----	49
Experimental Difficulties -----	52

<b>SIMULATION RESULTS</b> -----	56
Simulation 1 -----	56
Simulation 2 -----	58
Simulation 3 -----	59
<b>7. FUTURE DIRECTIONS</b> -----	<b>64</b>
<b>8. CONCLUSIONS AND RECOMMENDATIONS</b> -----	<b>65</b>
<b>REFERENCES</b> -----	<b>67</b>
<b>APPENDICES</b> -----	<b>70</b>
APPENDIX A: DERIVATION OF MODEL EQUATIONS -----	70
APPENDIX B: TEMPERATURE DEPENDENCE OF THE KINETIC CONSTANTS -----	74
APPENDIX C: MATLAB CODE -----	75
APPENDIX D: USING "FMINSEARCH" -----	85

## LIST OF FIGURES

Figure	Page
Figure 3.1: Schematic of a single reactor -----	12
Figure 3.2: Drawing of the main reaction -----	13
Figure 3.3: The Mechanism for the acetylation of salicylic acid -----	15
Figure 3.4: Illustrations of the automated laboratory reaction setup -----	16
Figure 3.5: Intelliform software for spectrograph acquisition and control -----	17
Figure 3.6: WinISO® software for controlling calorimeter reactor -----	19
Figure 3.7: graphical representation of raw spectra -----	23
Figure 3.8: Zoomed in view of the Figure 3.7 dotted rectangle -----	24
Figure 3.9: Plot of absorbance as a function of time -----	25
Figure 4.1: Plot of temperature of the reactor as a function of time steps -----	30
Figure 4.2: Graphical representation of the least-square method -----	33
Figure 4.3: Command flow diagram -----	36
Figure 6.1: Plot of Concentration Profiles as a function of time steps -----	41
Figure 6.2: Plots of Spectra for Exp. 5_01_03 -----	42
Figure 6.3: Surface Plot 1 of the Objective Function Value (J) -----	47
Figure 6.4: Surface Plot 2 of the Objective Function Value (J) -----	48
Figure 6.5: Zoomed in view of Figure 6.2 (a), Exp. 5_01_03 -----	49
Figure 6.6: Plot of Absorbance vs. Time Steps for Exp. 9_27_02 -----	50



Figure 6.7: Plot of Absorbance vs. Time Steps for Exp. 9_6_02-----	51
Figure 6.8: Plot of Absorbance vs. Time Steps for Exp. 1_10_03 -----	53
Figure 6.9: Plot of Absorbance vs. Time Steps for Exp. 1_10_03 -----	54
Figure 6.10: Plot of Absorbance vs. Time Steps for Exp.1_10_03 -----	55

## LIST OF TABLES

Table No.	Page
Table 6.1: Experimental results, kinetic constants .....	44
Table 6.2: Experimental results, initial Conc. of Water .....	45
Table 6.3: Experimental results, $V_{req}$ .....	45
Table 6.4: Constant Ratio Results .....	46
Table 6.5: Parameter values for Simulation 1 .....	57
Table 6.6: Parameter values for Simulation 2 .....	59
Table 6.7: $V_{req}$ values for Simulation 3 .....	62
Table 6.8: $k_2$ values for Simulation 3 .....	62
Table 6.9: $k_{1f}$ values for Simulation 3 .....	62
Table 6.10: $C_{W_0}$ values for Simulation 3 .....	63
Table 6.11: $C_{SA_0}$ values for Simulation 3 .....	63

## NOMENCLATURE

AA: Acetic Anhydride

SA: Salicylic Acid

ASA: Acetylsalicylic Acid

HA: Acetic Acid

W: Water

$C_Y$ : Molar concentration of species Y

$C_{Y_0}$ : Initial concentration of specie Y in the reactor

$N_Y$ : Moles of species Y

$N_{Y_0}$ : Initial moles of specie Y in the reactor

C: Matrix containing concentration profiles

A: Matrix containing spectra

$A_{est}$ : Estimated spectra matrix

$k_X$ : Kinetic constant for reaction X, [L/(mol \*min)]

$r_X$ : Rate of reaction X, [mol/(L \*min)]

ATR: Attenuated total reflectance

UV: Ultra Violet

HPLC: High Performance Liquid Chromatography

$V_{req}$ : Volume required to reach endpoint, [mL]

UV-VIS: Ultraviolet Visual

## 1. Introduction

In spite of their low volume, batch and semi-batch modes of processing are of great importance to the chemical industry due to their high value and high quality products such as pharmaceuticals, specialty polymers, cosmetics, specialty chemicals, biomaterials and pesticides. Batch processes are typically used when the production volumes are low, when isolation is required for reasons of sterility or safety, when the materials involved are difficult to handle (Srinivasan, *et al.*, 2002), and when regulations (such as those of the FDA) specify that commercial production methods must match development methods. Batch processes are characterized mainly by finite duration, non-steady-state behavior, and high conversion.

The traditional way of operating a reactor in a batch or semi batch mode is to follow a predefined recipe and to control manipulated variables such as temperature, pressure, and or pH along predetermined ideal trajectories; and only at the end of the batch it is determined if the product has the required qualities. Often disturbances or natural variations in loading conditions (such as impurities in the reactants) or the change in operating conditions or calibrations can go undetected and cause the variables to deviate from their optimal trajectories, which may adversely affect product quality. Chemical composition of the product is the most sought after quality. However, accurate chemical information is mostly obtained by off-line analyses, and in many cases the time for analysis exceeds the batch time. Therefore, chemical analysis can only be used after the

batch is complete, which is too late for any corrective action to be taken on previous batch and only the subsequent batches can benefit from the information (if subsequent batches sustain the same new behavior).

Therefore, a batch monitoring and optimization system that can acquire composition information in real-time and track the evolution of a batch, detect variations and revise the optimal recipe on-line, is needed to allow corrective measures to be taken early in the batch and to ensure safe operation, required product quality, and minimal in-batch time.

The use of in-situ spectroscopic measurement as a non-invasive on-line method for extracting chemical information has received significant attention in the past few years. The classical curve resolution (CCR) algorithm is one such method, which uses spectrometric data along with a chemical model to obtain the chemical composition profile (Bijlsma, *et al.*, 2000).

To the best of the author's knowledge, this method has not yet been used for the characterization of a batch titration system in which the initial concentrations of the batch charges are not known. This type of scenario often occurs in the chemical waste treatment industry; often some (or all) species in a waste stream may need to be neutralized before disposal but their exact composition is not known. This type of scenario can also occur when the batch is fed by an up-stream process or from natural materials and the feed concentration is variable from batch to batch.

The main idea of this thesis is to show that the volume of reagent needed to reach a batch endpoint (reaction completion, when initial reactant has been completely consumed) can be predicted on-line in and real time. By monitoring the reactor's time-dependent

spectroscopic response, after a few small additions of one of the reacting reagents, the kinetic model will be adjusted online. The adjusted model will be then used to determine the stoichiometric quantity of reagent exactly needed to complete the reaction. Large reagent additions of the right amount can then be confidently/safely made to reach the endpoint rapidly, thereby shortening the batch time without wasting reagent, thereby improving yields reducing separation cost and reducing impurities in finished batches.

The author of this thesis has developed a software code, based on the CCR method mentioned previously, that receives spectroscopic data from a batch reactor and uses that to parameterize the kinetic model. Once a viable chemical model is identified, it is used to predict the amount of reagent required to reach the end-point of the batch. All of this is done without requiring any knowledge of the initial concentration of the reactants; in fact it does not require knowledge of the actual concentration time profiles of either the reactants or the products. The applicability of this software as an online tool for predicting volume necessary to reach endpoint is shown by using simulation experiments as well as lab-scale batch reaction experiments.

## 2. Background

Optimization of batch processes has been the focus of many studies (Love, 1988, Bonvin, 1998). Due to the non steady-state nature of batch processes there is no setpoint around which the key variables can be regulated. Process variables need to be adjusted with time. The main goal in batch operation is not to keep process variables at some optimal constant setpoints, but rather to optimize the recipe (addition times, addition amounts, temperature and pressure schedule, agitation events, etc) to maximize performance.

Though potential gains of optimization could be significant, there have been only a few attempts to optimize operations through mathematical modeling and optimization techniques. Instead, the recipes developed in the laboratory are implemented conservatively in production, and the operators use heuristics gained from experience to adjust the process periodically, which may lead to a slight improvement from batch to batch (Wiederkehr, 1998).

### **Off-line Optimization**

Techniques for batch-to-batch recipe optimization, a type of off-line method of batch optimization, have been shown to work in maintaining product quality (Dong, *et al.*, 1996). In this type of optimization knowledge obtained from previous batches is used to update the recipe. However, since all deviations that might occur cannot be predicted before the beginning of a batch, corrective action cannot be taken while the batch

progresses, thus this technique cannot be used to improve the current batch. This is the main disadvantage of all off-line optimization techniques. (Zafirio and Zhu, 1990)

### **On-line Optimization**

With contemporary computer processing power, on-line batch optimization based on on-line measurements has interested a lot of researchers in the last decade (Eaton and Rawling, 1990; Soroush and Kravaris, 1992; Choi, *et al.*, 1997; Ruppen, *et al.*, 1998; Dhir, *et al.*, 2000).

### **Model Based Optimization**

There are two main types of models, namely empirical and first-principles, that are used in the industry for control and optimization of batch processes. Further subdivision in these two types also exist but is not described here, for further details on these subdivisions refer to (Bonvin, 1998). Future evolution of the batch cannot be predicted without a model that accurately represents the process under consideration. Many optimization studies on batch processes, especially fermentations and polymerization, are based on the use of process models (Johnson, 1998).

#### ***Empirical Models***

Types of models are purely data driven, and abnormal variations are identified in terms of maximum variance in the data. Because of their simplicity and ease of automation, these methods are widely used in the process industry. Automation of process plants has increased the potential of these types of data driven approaches. Most industries maintain a fully automated historical database of process conditions and measurements such as temperature, pressure, flow rate, and product quality etc., which provides enormous



amount of information regarding the process. Historical data is used to find general trends of the process conditions, which has been proven to have produced good results such as on specification product quality and safe operation, is known and is used to develop the relationship between process variables and product quality.

This database of information is the backbone of empirical models; therefore, these models are only as good as the data available to them, and cannot be applied to new process without requiring time consuming data acquisition and extensive training. Also, they cannot be used to understand the underlying physicochemical cause of variation in the conditions of a process, thus limiting the further understanding of the process. Due to their data driven structure they show poor extrapolation properties. Empirical models thus can only be used, quite successfully, for control purposes but not for further optimization of the process.

Multivariate statistical procedures for monitoring the behavior of batch processes are an example of use of empirical models. Boqué, *et al.* (1999) use multiway covariates regression on historical data to find relationships between process variable and quality variables of the final product. On-line predictions of the final quality variables are monitored to assure the on-spec product. This type of method requires historical data from successful batches and extensive training.

### ***First-Principles Models***

First-principles models are based on scientific knowledge such as mass and energy balances, reaction kinetics, stoichiometry, transport phenomena, etc. Although a first-principles approach has a very ambitious goal to model real systems using few approximations (or none at all), they can be very reliable. A cause of deviation in the

process conditions can be easily pinpointed using such models, and extrapolation can also be done accurately. The complexity of the process being modeled is the main deterrent in the use of this type of models. The need for finding the parameters, to make the model accurately represent the process is another somewhat difficult requirement. For examples of first principles models being used for optimization refer to Agarwal (1997) and Abel, *et al.* (2000).

Models (i.e. empirical and first-principles models) described above could be of two types, they could either be fixed or adaptive. Fixed models used fixed parameters found in the developmental stage, they need to be fairly accurate thus can only be used with very well understood systems. Adaptive models are mostly used when a detailed model is not available, real-time re-parameterization of the partial model may be used to accurately define a process within a short interval of time (if not for the whole time range). In one experimental optimization of a batch process, the parameters of a simple unstructured, un-segregated first principles model were dynamically adjusted to maintain an accurate representation of the process (Iyer, *et al.* 1999). Once the model parameters were adjusted, the batch was re-optimized, whereby inaccuracies in the model were taken care of by on-line data reconciliation and model parameter adjustment. Although that work focused on a fed-batch fermenter, the approach is perfectly general and is easily applicable to any batch process that can be modeled. Refer to Srinivasan, *et al.* (2003), Bonvin (1998), Bonvin (2003), and Le Lann (1998) for more information on model based optimization techniques.

## **Model Free Optimization**

The main idea is to use measurements directly without any help of a process model. Since the technique being discussed in this thesis is a model based approach, model free optimization will not be discussed any further (for more detail on this method, refer to Srinivasan, *et al.* (2003), Bonvin (1998), and Bonvin (2003) and for examples on the use of this method refer to Terwiesch and Agarwal (1994), Van Impe and Bastin (1995), and Soroush and Karavaris (1992)

## **Chemical Analysis Tools**

Accurate chemical composition information is obtained mostly by off-line analyses, and in many cases the time for analysis exceeds the batch time. In most cases off-line analyses do not accurately reflect the composition of the batch mixture at the time of sampling, for example reference data obtained by HPLC analysis requires the quenching of the reaction mixture which usually destroys reactive intermediate. Therefore, chemical analysis can only be used after the batch is complete, which is too late for any corrective action to be taken on previous batch and only the subsequent batches can benefit from the information. Since the technique being discussed in this thesis uses an on-line analysis tool (real time spectroscopy) no further discussion on different types of off-line analysis tools is provided here.

## Spectroscopy

The use of in-situ spectroscopic measurements as a non-invasive on-line method for extracting chemical information has received significant attention in the past few years (Gemperline, *et al.*, 1999, Quinn, *et al.*, 1999, Bijlsma, *et al.*, 2000, Bezemer, *et al.*, 2001). Near infrared spectroscopy, short-wavelength near-infrared spectroscopy and ultraviolet visible spectroscopy are commonly used for monitoring chemical reactions (Burns *et al.* 1992, and Workman, 1996). All these methods use some sort of curve resolution algorithm to find composition profiles.

Curve resolution techniques to find kinetic constants have been in use since the early 70's and have become very popular. If spectra have been obtained during a batch, and the kinetic equations are available then curve resolution methods can be used to estimate reaction rate constants as shown by Lawton (1971) and by Sylvestre, *et al.* (1974). Basically, there are two main types of curve resolution techniques: iterative and non-iterative. Iterative techniques are slightly slower but more accurate than non-iterative techniques, non-iterative methods produce biased estimates when only moderate signal to noise ratio is present in spectroscopic data.

Bijlsma, *et al.* (1998) describe two different curve resolution techniques that use SW-NIR (short wave near infrared) measurements to predict reaction rate constants. One of these techniques is non-iterative. Although fast, it only gives rough estimates of the reaction rate constants. It is based on the generalized rank annihilation method and is sensitive to noise. The second technique is an iterative algorithm, based on Levenberg-Marquardt algorithm and alternating least squares optimization. It gives more accurate results than does the first technique, but requires the results of the first technique as initial guesses.

Classical curve resolution (CCR) algorithm which uses spectrometric data along with a chemical model to obtain the chemical composition profile has been shown to work successfully (Bijlsma, *et al.*, 2000). In this study UV/Visible spectroscopy has been used to monitor a biochemical reaction. This technique does not require pure species spectra. Minimization is done by Levenberg-Marquardt algorithm.

### **End-Point Determination:**

To the best of the author's knowledge no one has worked on identifying the material required, stoichiometrically, to completely react all the batch material (referred to as the end-point) online, specifically fed batch reactors. A lot of research has been done on finding end-point of titration experiments, but they do not predict the end-point they merely identify it after it has occurred.

### 3. Experimentation

This section has been adapted from Shane S. Moore's thesis. The project under consideration is a collaborative venture between the School of Chemical Engineering at Oklahoma State University (OSU), Stillwater, Oklahoma and the Department of Chemistry at Eastern Carolina University (ECU), Greenville, North Carolina. Shane Moore, an MS student at ECU, is the person who conducted the experiments under the guidance of Dr. Paul J. Gemperline.

#### **Introduction**

In order to make an accurate prediction using updated parameters and maintain control of the batch reactor system, a simple reaction was used. The reaction follows an  $A + B \rightarrow C + D$  mechanism, with one of the reactants and one of the products having unique UV/Visible absorbances. Each batch titration is a separate process implemented through an experimental design with slightly different conditions to give robust results.

The batch recipe being taken under consideration here is the production of aspirin (acetylsalicylic acid, ASA). The process being modeled in this project is shown in Figure 3.1. The reactor system consists of a 50 ml reactor vessel that fits in a glass jacket. The cooling jacket and the heating coil are used to maintain isothermal conditions, and the stirrer for uniform mixing. Batch monitoring is done by the use of fiber optic UV/visible attenuated total reflectance (ATR) probe.

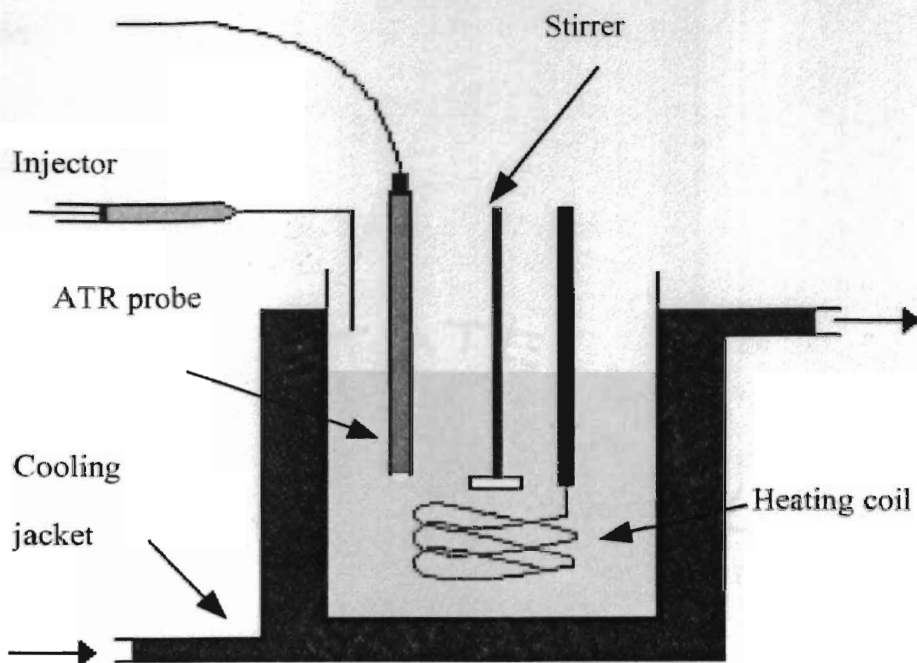


*Figure 3.1: Schematic of a single reactor*

The reaction used is the esterification of salicylic acid (SA) to form acetylsalicylic acid (ASA). This reaction system was chosen as it is well known, and is widely used in the industry.

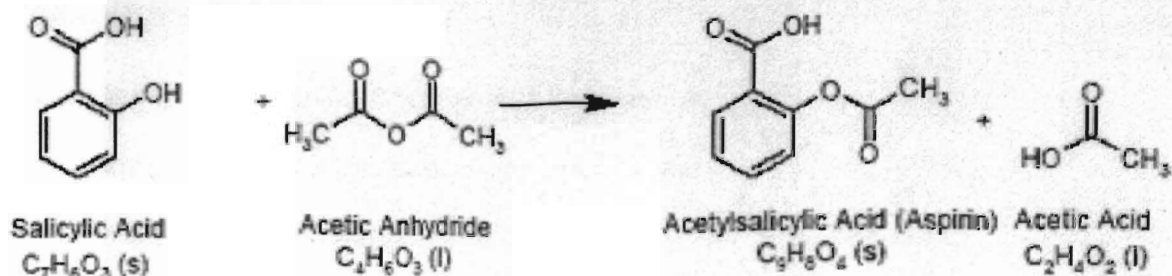


**Figure 3.2: Drawing of the main reaction**

Source: [http://courses.chem.psu.edu/chem14/FormsF03/aspirlab2\\_F02.pdf](http://courses.chem.psu.edu/chem14/FormsF03/aspirlab2_F02.pdf) (10/15/03)



In Reaction R1, shown in Figure 3.2 SA reacts with AA to give, ASA and acetic acid (HA). Reaction R2 is an undesired side reaction, which occurs between the contaminant water (W), present in the reaction mixture introduced to the system by absorption from the atmosphere and or as residual from the apparatus cleaning procedure, and the AA being added and gives HA.

After the Reactor is filled with acetonitrile (solvent of choice), a measured amount of powdered salicylic acid (SA) is added and allowed to time to mix, a small quantity of acetic anhydride (AA) is injected. One of the reactants, SA, and one of the products, ASA, are the only reagents in this system that show unique UV/Visible absorbance.



## **Reaction Mechanism**

Solid salicylic acid dissolved in a solvent reacts with liquid acetic anhydride to form the acetylation products acetylsalicylic acid (aspirin or ASA) and acetic acid. A catalyst is added to speed up the reaction. Figure 3.3 illustrates the mechanism (Walter 1996) of the acetylation of salicylic acid. There are three steps involved to get to the ASA product. The first step is the formation of a tetrahedral carbonyl addition intermediate with the electron pair from the O-H group attacking the C=O group. The next step is a proton transfer from the O-H group to regenerate the C-O group. The last step involves the formation of the ASA product and acetic acid by breaking of the C-O bond.

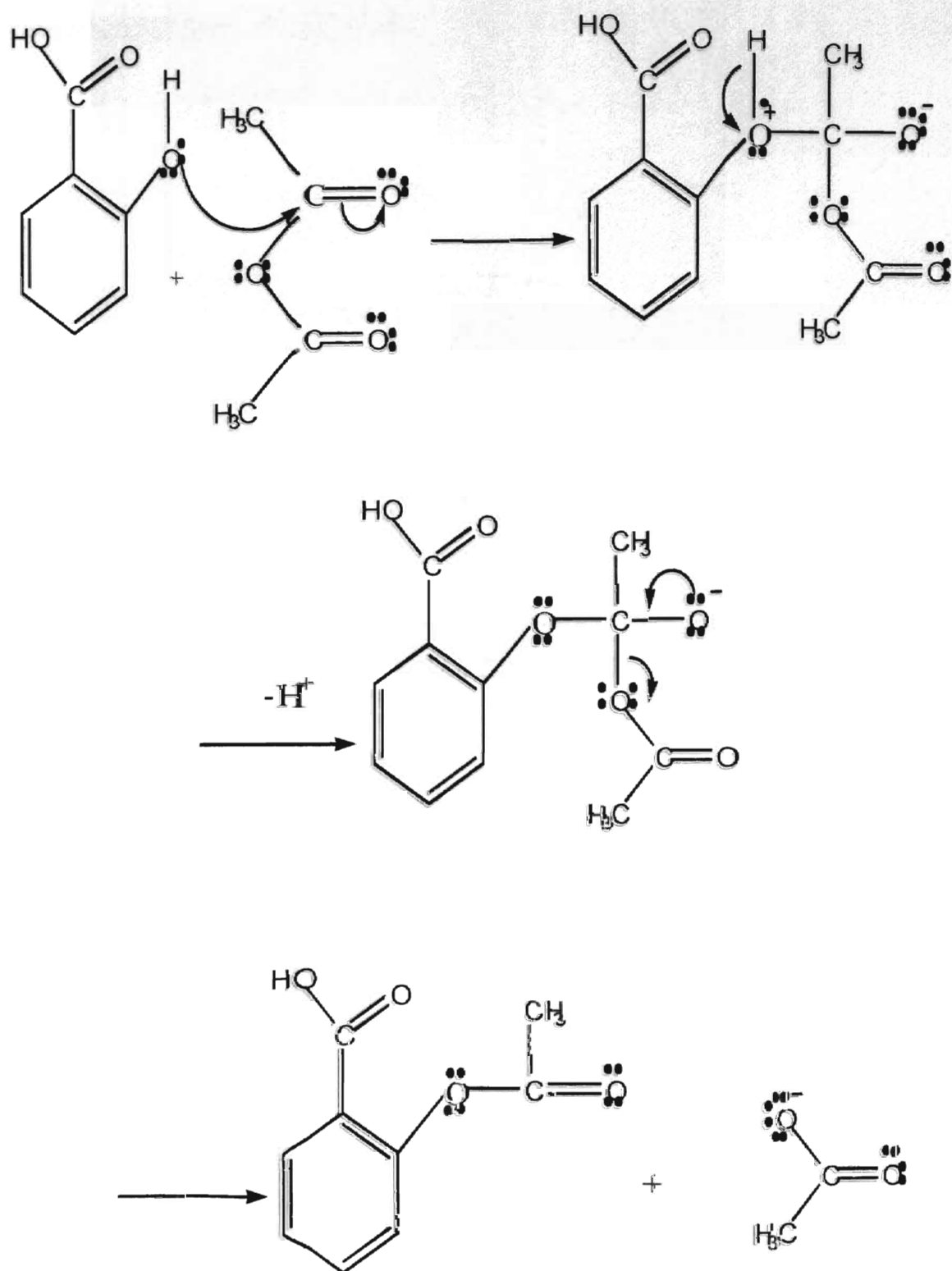


*Figure 3.3: The Mechanism for the acetylation of salicylic acid*

## Data Acquisition and Control

A schematic of the real-time automated laboratory reactor set-up is shown in Figure 3.2.

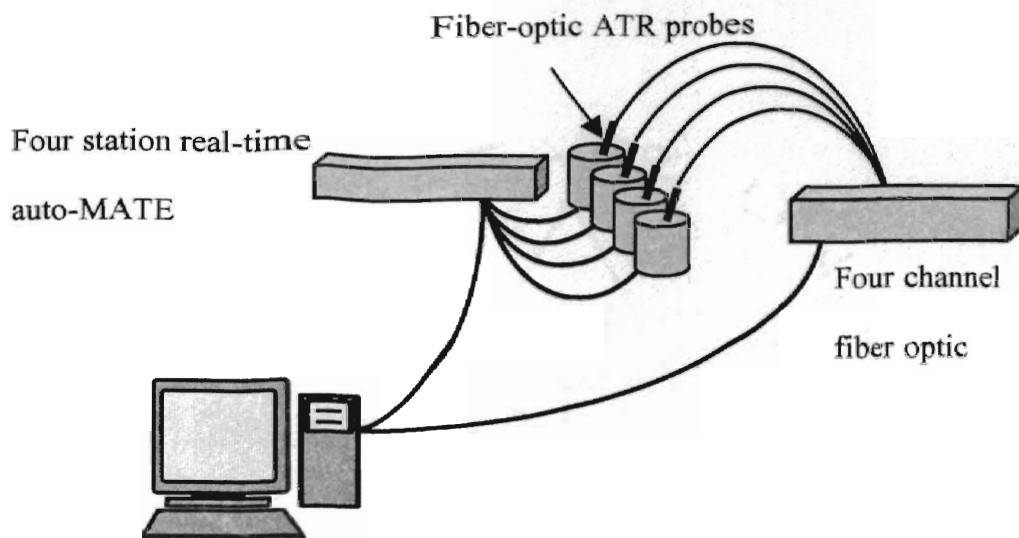


*Figure 3.4: Illustrations of the automated laboratory reaction setup*

IntelliFORM®, developed by H&A Scientific, Inc., controls the spectrograph and gives spectroscopic analysis of batch runs while WinISO®, developed by H.E.L. Ltd, controls the automated reactor and calorimeter. IntelliFORM® (Intelligent Fiber Optic Reaction Monitoring, H&A Scientific, Inc., Greenville, NC) is a Microsoft Windows® application software package that can analyze batch reactions to determine component concentration, formation of products, and reaction rate. IntelliFORM® has four channels capable of collecting spectra depending upon how many reactors are being used.

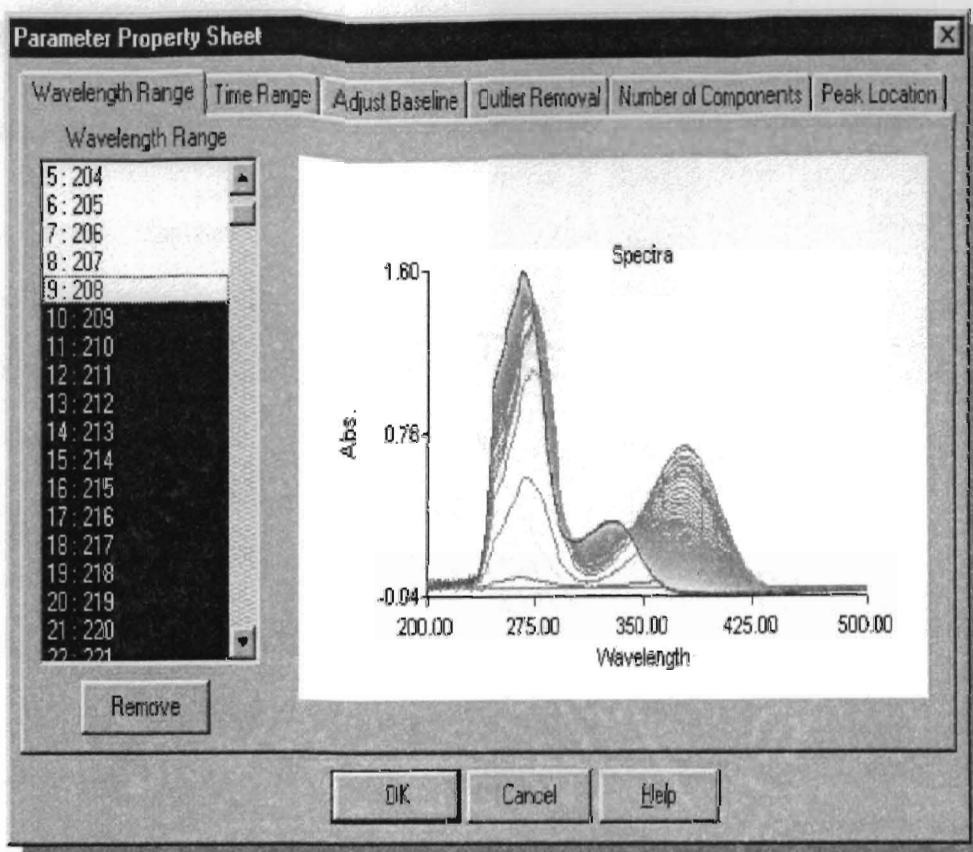


**Figure 3.5: Intelliform software for spectrograph acquisition and control**

IntelliFORM® when coupled with fiber optics, a UV/Visible spectrograph, and a real-time automated laboratory reactor forms a complete reaction station capable of characterizing batch reactions. IntelliFORM® can characterize batch reactions without taking reference measurements and give valuable information on reaction rate and progress in real time.

## **Instrumentation**

### **Calorimeter System**

An auto-MATE 4-vessel miniature automated reaction calorimeter system was used for all reactions (Hazard Evaluation Laboratory Limited, Hertfordshire, England and H&A Scientific, Inc., Greenville, NC). The auto-MATE reactor system is computer controlled for optimization of batch reactions. It has features of industrial scale reactors and robotic systems. Experiments can be performed under realistic conditions, fully automated and controlled. Each of the four reactors runs independently under control from a single computer. The reaction conditions are monitored simultaneously with control of all parameters (i.e. jacket temperature, internal reactor temperature, stir rate, reagent flow rate, reagent feed times). With the use of Chemometric methods, this automated laboratory reactor system can be used to integrate differing types of measurements such as spectroscopy, temperature, and calorimetry into one mathematical calibration and process model.

Each reactor has a 50 mL glass reactor vessel that fits in a glass jacket filled with oil from a heater/chiller circulator. The reactor is separated from the reactor head, which contains six ports into the reactor: (1). Overhead stirrer, (2). Thermocouple, (3). Coiled reactor heater, (4). UV/Vis ATR probe, (5). Solid addition port, (6). Liquid addition port. The top and reactor vessel are clamped together to form a gas tight seal. The heater/chiller is a Julabo F25 oil circulator connected by rubber hoses to the glass jackets in series. The reagent delivery pumps are Harvard Apparatus mechanical pumps supplied by H.E.L. Ltd. Glass syringes sit on top of the pumps, which push the syringe to dose the correct amount based on the diameter of the pump. The WinISO® software is the control

platform for the reactor system. It is a Windows based program designed to control hardware and acquire data from the reaction calorimeters (H.E.L. Ltd). The program collects data in real-time in the form of graphs and stores the data in a spreadsheet form. The user interface is illustrated below.

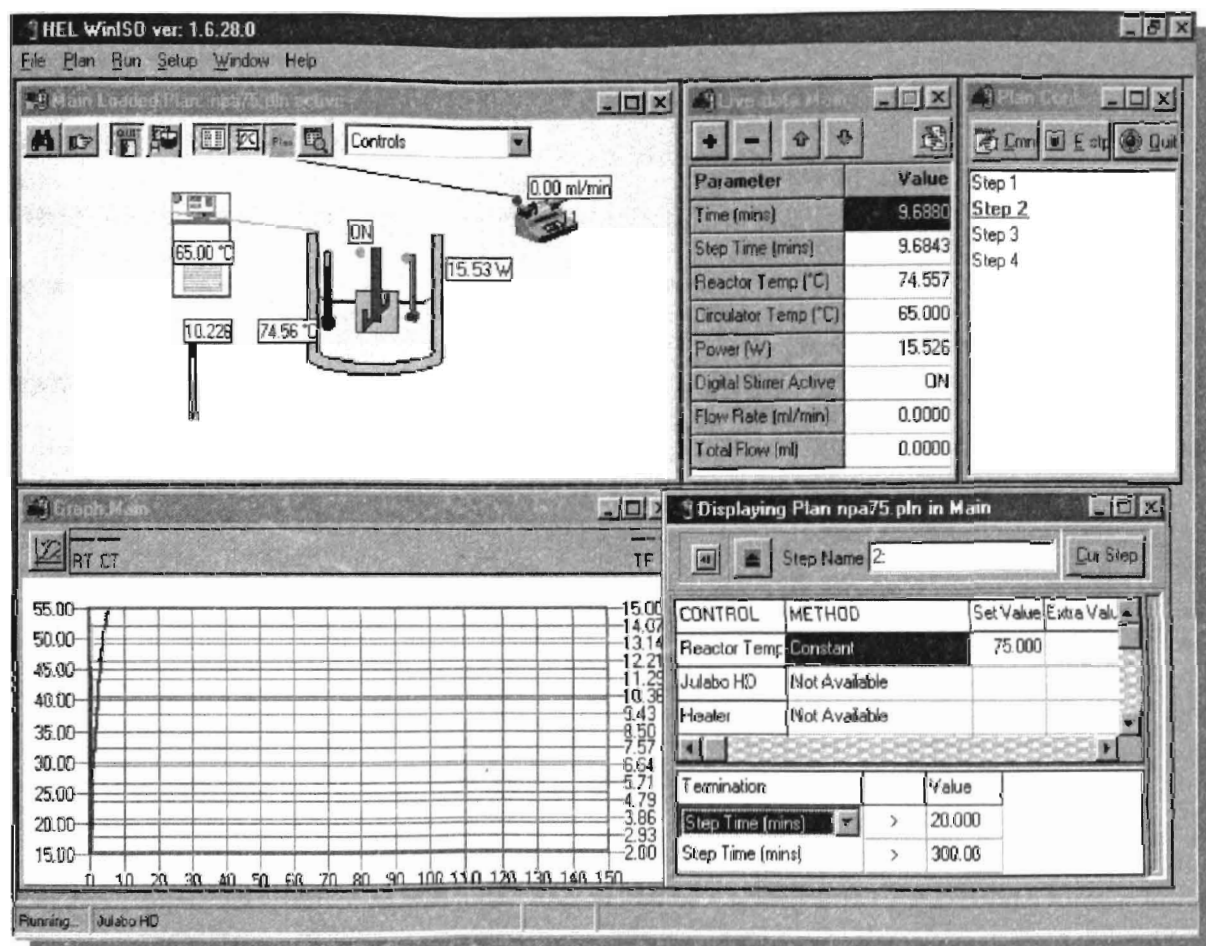


**Figure 3.6: WinISO® software for controlling calorimeter reactor**

It shows the reactor controls, real-time data acquisition, the current conditions, and the reaction plan details. The reaction plan consists of a series of precisely timed steps. The software controls the beginning and ending time of each step.

Reactions were run in airtight conditions, to eliminate sources of error from heat lost through the heat of evaporation. Prior to a reaction, the reactor is pressurized to about 5 psi with dry nitrogen to insure that it has a gas tight seal. Once the reactor is set up and charged with the initial reagents, a plan is created in the WinISO® software. This project used nine steps in the reaction plan. Before the reagents are added, the stirrer, heater, and oil bath were turned on and allowed to reach steady state conditions. After the nine steps are completed, the experiment terminates and the all of the data is saved in a predetermined file on the computer. Details about the plan used in this project are given in section 3.5.

### **UV/Vis Fiber-optic CCD spectrometer**

A multichannel fiber optic CCD UV/Visible spectroscopy system (Equitech International Corp., Aiken, S.C.) used for making all *in-situ* spectroscopic measurements. The system consists of a Millennium 3 (M3) UV/Visible spectrophotometer, a Xe flash lamp as the light source, internal optical fibers and power supplies all contained within a rack-mount box. The spectrophotometer is designed for the simultaneous imaging of 400-micron core input fibers onto the detector array. It has a wavelength range of 190-790 nm with a dynamic range greater than 50,000 and S/N of 20,000:1. The probes used were attenuated total reflectance (ATR) probes, capable of operating over a wide range of temperatures, from -50° C to 300° C and at pressures up to 1200 psi. The probes are encased in a stainless steel shaft (1/4" x 4"), which protects the fibers from the reaction environment.

At the end of the probe is a three-bounce sapphire crystal. The light enters through the input fiber and bounces on the crystal and back into the output fiber traveling to the

detector and CCD array. However, the electromagnetic energy from the light penetrates slightly beyond the crystal surface producing the so-called evanescent field. This field extends about 1.5 microns beyond the crystal surface. Absorption by the sample occurs in this evanescent field near the crystal surface. The probe only needs to be submerged enough to cover the crystal in the solution. The light not absorbed is sent back to the detector through the output fiber. The less light received is measured and recorded on the spectrometer. Sapphire allows response down to 220 nm in samples with an index of refraction up to 1.5, as well as offering excellent resistance to chemical attack.

The fibers are composed of two 400-micron core fused silica fibers spaced opposite each other in a semicircle around the circumference of the ATR hemisphere crystal. There is an input fiber and an output fiber positioned 180° from each other. The probe is constructed so that it requires no internal optical elements other than the ATR crystal. The probe is simple to manufacture and is more rugged than possible with a complex optical design.

Spectra were collected in the process every six seconds. Six seconds was chosen because a fast collection time was needed to get the most accurate picture of the system over the reaction process. The computer needed time to process the data collection and display the spectra on the screen. Collection of spectra faster than 6 seconds was found to be more than the computer could handle. Before a reaction was started, the intensity of light reaching the CCD detectors was evaluated. A good CCD image from the probe gave an intensity of about 50,000 counts. IntelliFORM® allows the user to adjust the CCD integration time, the flash lamp duration, and number of pulses, so the intensity of the light reaching the detector matches the fiber-optic probes light throughput characteristics.



The intensity was adjusted before each batch to let the maximum light amount in (50,000 counts) while not overloading the detector. The control of the integration time is called the instrument trigger. The number of exposures and the trigger period were adjusted to improve instrument performance. After the intensity setting was optimized, a blank spectrum of the reactor components was taken so data acquisition could begin.

The collection of spectra is set up in two steps. The first step is a 1.5-hour wait time for the drift to disappear in the spectra while the SA is dissolving. During this time the probe is placed inside the reactor in contact with the initial solution of SA and acetonitrile at thermal equilibrium. During this time the spectra are being collected at an interval of two minutes. Fast collection times are not needed during this wait time because no reaction is taking place. The second step was to collect spectra every six seconds during the reaction. This project requires analyzing the spectra during a run. IntelliFORM® has the capability to save the collected spectra during any point in the reaction in a temporary file. This file can be transferred to another computer over a network and opened with IntelliFORM® to analyze specific time ranges. All of this happens without pausing or stopping the data acquisition.

## Spectra Processing

An example of the whole spectra, as received via the UV/Visible ATR probe placed inside the reaction mixture, recorded during an experiment is shown in Figure 3.7. Analyzing the full range of wavelength (200 nm to 800 nm) is not necessary only information inside the dotted rectangle in Figure 3.7 of use. Outside the 260 nm to 350 nm wavelength range, either none of the species absorb, or the change in absorbance caused by the change in concentration is very small causing a high noise to signal ratio.

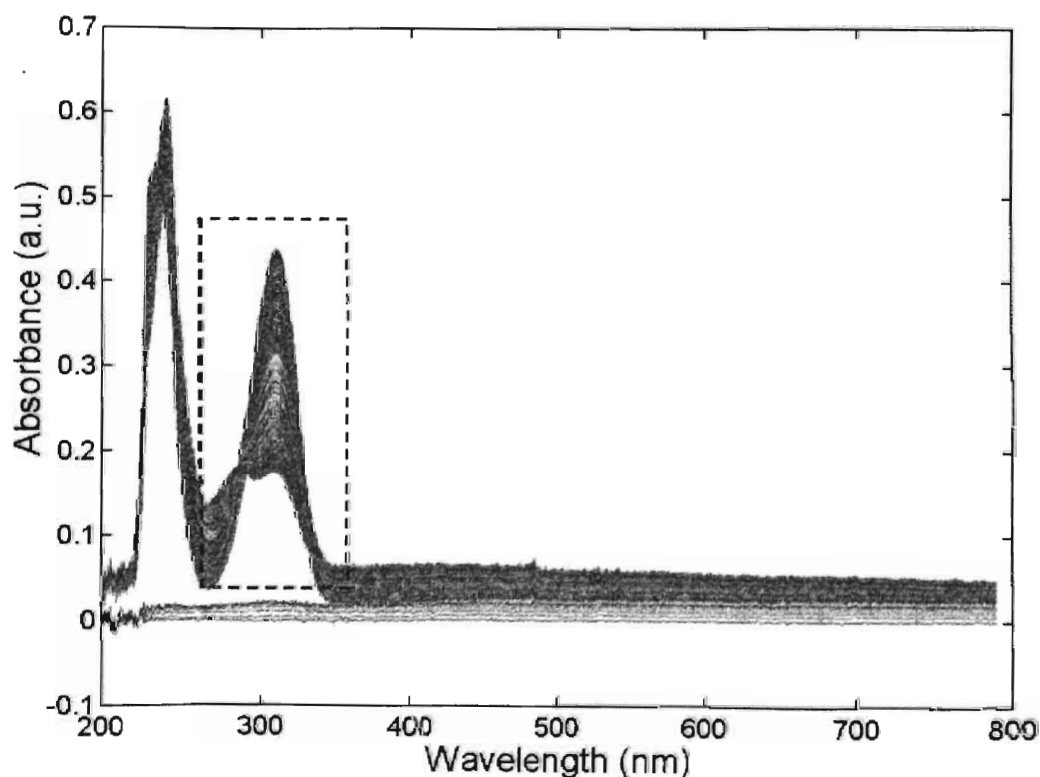


*Figure 3.7: graphical representation of raw spectra*

Figure 3.8 shows the zoomed in view of this region (260 nm to 350 nm). The arrows indicated the direction of change in absorbance with time. Since one of the reactant and

one of the products shows unique UV absorbance one peak can seen dropping and one peak rising with time during an experiment. Only information from this range is used by the algorithm.

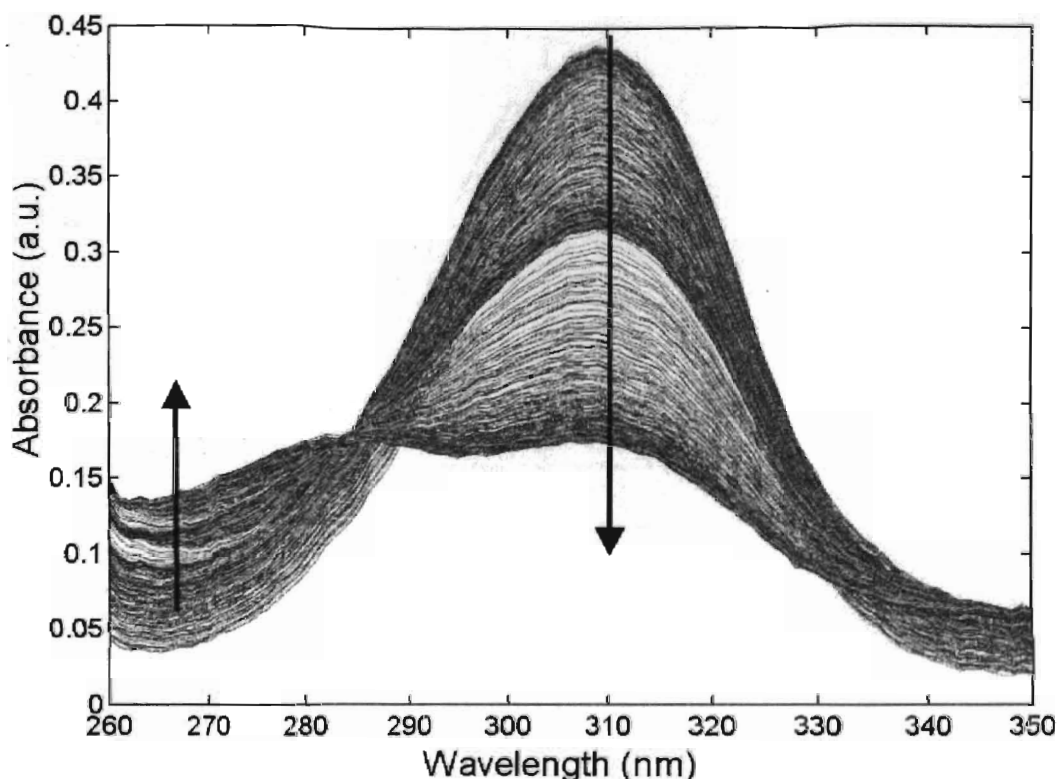


*Figure 3.8: Zoomed in view of the Figure 3.7 dotted rectangle*

Figure 3.9 shows the same information but with time as one of the axes. Each line represents a different wavelength. It can easily be seen that absorbance at some wavelengths is rising and dropping at some representing the depletion of the absorbing reactant and production of the absorbing product. The CCR algorithm requires that the spectra be fed in the form of absorbance as a function of time which shown in Figure 3.9

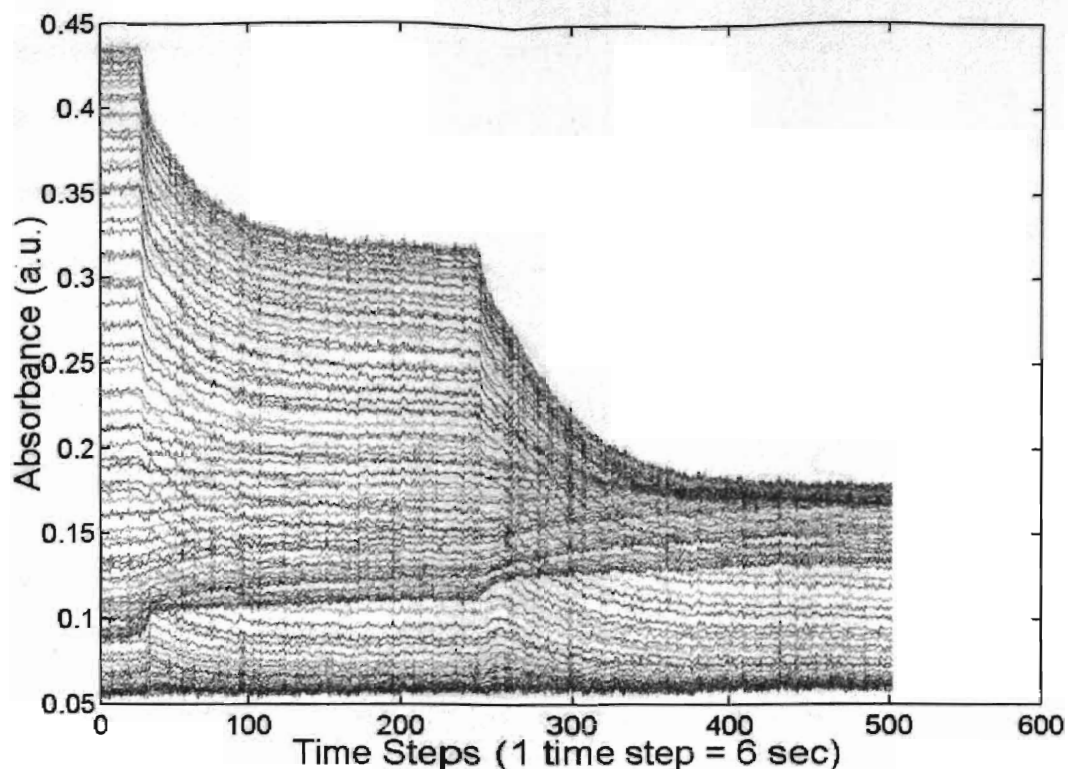


*Figure 3.9: Plot of absorbance as a function of time*

### **Reaction Conditions**

The reaction was reduced from an industrial scale to a laboratory scale. The reactor is a 50 mL glass reactor. The solvent used for the reaction is acetonitrile and the catalyst used was sulfuric acid. It was suspected that sulfonated compounds were formed by interaction with the products. Later investigations by electrospray LC-MS proved this hypothesis false. 25 mL of acetonitrile was used as the solvent with 0.2 mL of concentrated sulfuric acid (Fisher Scientific, NY) as catalyst for each batch. This was the initial reactor charge in the real-time auto-MATE reactor vessel (Hazard Evaluation Laboratory Limited (H.E.L. Ltd.), Hertford, England).

In this project each batch reaction had nine steps under software control. The first step was an equilibration step. At this point the plan was started and the initial charge heated to 60° C. This initial equilibration step was necessary to achieve constant reactor and circulator temperature prior to the addition of reagents. This step lasted for 20 minutes. Near the end of this step when the initial charge was maintained at 60° C, a blank was taken with the UV/Visible spectrograph. This blank was used as a reference spectrum for all remaining spectroscopic measurements. Once started, the spectrograph was set up to collect spectra at the same rate as the WinISO software.

A precisely measured amount of salicylic acid (Fisher Scientific, NY) of 2 to 4 grams was added to the reactor vessel in powder form after the blank was taken. This was the second step of the plan and lasted for two minutes. The third step was an equilibration step for the SA to dissolve and for the system to come back to steady state conditions. It is hypothesized that the SA when in solution weakly adsorbs to the surface of the ATR crystal, causing the spectra to drift with increasing absorbance, further research is needed to validate this hypothesis. The SA over time reaches a saturation point after about one hour and no longer causes drift. The equilibration step was programmed to last for about one and a half hours to give the probe time to equilibrate and for the drift in the spectra to disappear.

After the salicylic acid was completely dissolved at a constant 60° C temperature, the titration with acetic anhydride (Fisher Scientific, NY) was started. This was the fourth step in the plan with a wait period of about 20 minutes after each addition as the fifth step. The auto-MATE reactor syringe pumps carried out the additions. The fourth and fifth steps were repeated to give as many AA additions as required. The metered doses of

AA were used in the reaction. The doses were added drop wise through a tube directly into the reactor at a specified rate controlled by the WinISO software. The flow rate was slow (0.50 mL/min) in order to make the additions more accurate. The slower the rate the less the pumps will overshoot the needed amount. WinISO recorded the actual amount of acetic anhydride delivered. There was a wait time between the additions in order for the system to come back to equilibrium and to make sure that there was adequate information in the spectra to use in the kinetic models for the prediction of the endpoint.

## 4. The Algorithm

This is an iterative curve resolution method combined with non-linear fitting.

### Algorithm Basis

According to the Beer-Lambert law, there is a linear relationship between the concentration of a species and their molar absorptivity which can be described by

$$a_{\lambda} = c_1 \times e_{1\lambda} + c_2 \times e_{2\lambda} + \dots + c_n \times e_{n\lambda} \quad (4.1)$$

In summation form this can be written as

$$a_{\lambda} = \sum_j^n c_j e_{j\lambda} \quad (4.2)$$

If concentration changes in time, then  $a_{\lambda}$  will be dependent on the  $t^{\text{th}}$  sampling and the set of equation (4.2)s can be written in matrix notation as

$$\mathbf{A}(t \times m) = \mathbf{C}(t \times n) \cdot \mathbf{E}(n \times m) \quad (4.3)$$

Where

$\mathbf{A}$   $\equiv$  matrix of absorption as a function of reaction time  
 $\mathbf{C}$   $\equiv$  matrix of concentration as a function of reaction time  
 $\mathbf{E}$   $\equiv$  matrix of absorption as a function of reaction time for pure species spectra  
 $\lambda$   $\equiv$  wavelength

$a_{\lambda}$   $\equiv$  overall absorbance at wavelength  $\lambda$   
 $c_j$   $\equiv$  concentration of specie  $j$   
 $n$   $\equiv$  total number of absorbing species  
 $m$   $\equiv$  total # of wavelengths  
 $t$   $\equiv$  total # of equidistant time points  
 $i$   $\equiv$  total # of absorbing species  
 $e_{j\lambda}$   $\equiv$  molar absorptivity of specie  $j$  at wavelength  $\lambda$

## **Algorithm**

The relationship between the data received from the probe (matrix **A**) and the time dependant concentration profile is given by Equation 3.3. If **E**, the pure species spectra matrix, is known, then **C**, the concentration profile matrix, can be easily calculated. But, to find **E**, the probe needs to be calibrated with standard solutions such that their concentrations match the initial concentration of the absorbing reactants and the final concentration of the absorbing products of every batch experiment to be performed, which is impractical. Without **E**, **C** cannot be directly found.

The CCR method suggest a way around having to find **E**. According to the CCR method, model parameters (e.g. initial concentrations and kinetic constants) can be assumed and the concentration profiles ( $C_{\text{mod}}$ ) can be generated by using a kinetic model representing the reaction system under consideration given below.

## **Kinetic Model**

Model equations were developed based on traditional mass balance assuming an isothermal batch. The experiment is conducted nearly isothermally, as shown in Figure 4.3. The first peak labeled as "1<sup>st</sup> Addition" in Figure 4.3 is caused by the addition of the first aliquot of AA, and since SA and AA and W and AA react exothermally (W and AA more so than SA and AA) rise in temperature can be seen, but this exotherm last for a very short time as compared to the reaction time due to the rapid heat loss to the cooling jacket, and also the magnitude is very small only a change of about 0.4 °C. The 2<sup>nd</sup> addition shows an initial drop in temperature, this is because there is lesser amount of SA and W left to react after the first addition therefore less heat is produced, and because



aliquot added is at room temperature (about 25 °C). The rise is caused by the heater being turned on by the controller. All other additions show a similar behavior. Although there are some variations in the temperature the change in temperature and the duration of the change were very small; therefore, the temperature dependence of reaction rates is not modeled. Detail on the temperature dependence of reaction rate constant can be found in Appendix B.

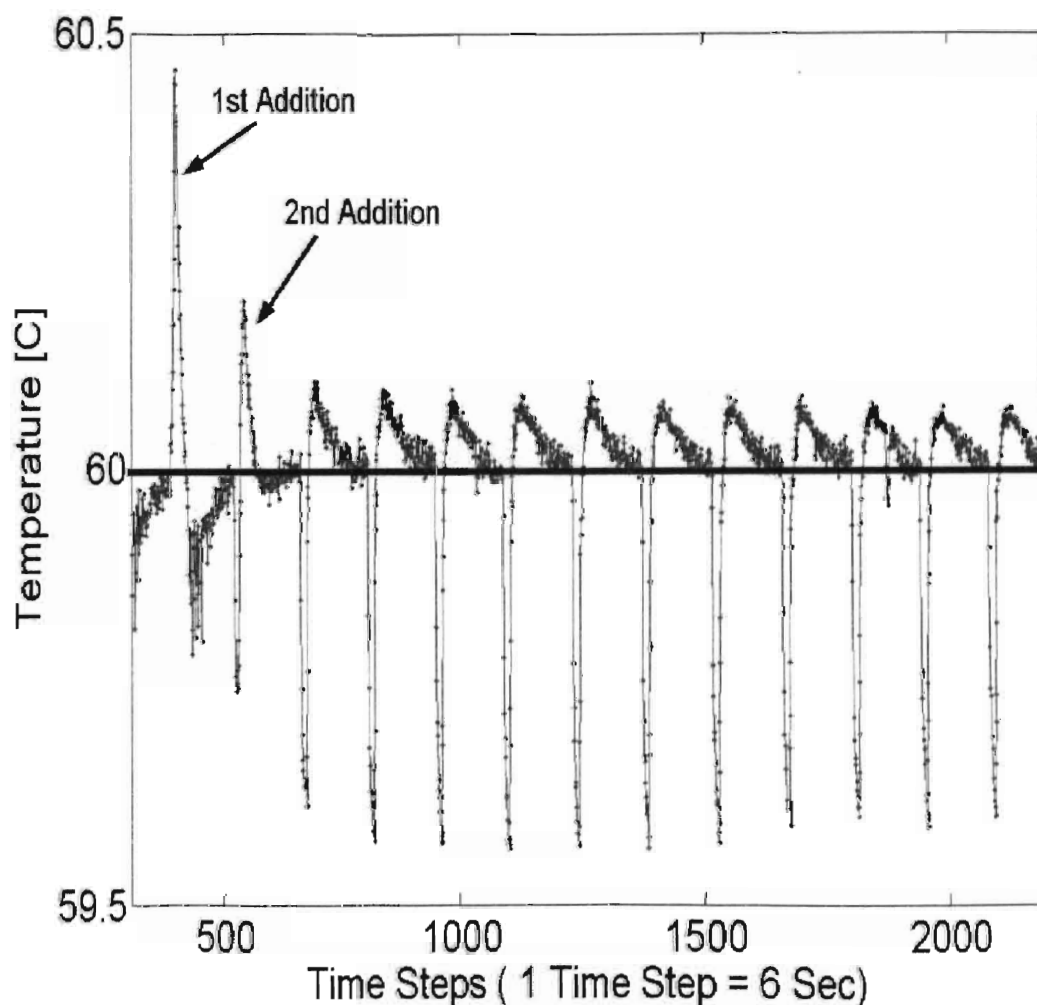


*Figure 4.1: Plot of temperature of the reactor as a function of time steps*

The kinetic model is based on the most dominant reactions occurring in the system



This reaction system is a well known system with known reaction rate laws.

$$r_1 = k_1 C_{SA} C_{AA} \quad (4.3)$$

$$r_2 = k_2 C_{AA} C_W \quad (4.4)$$

where

$k_{\#} \equiv$  kinetic constant for reaction R#

$r_{\#} \equiv$  rate for reaction R#

$C_Y \equiv$  concentration of species Y

The general mass balance equation is

Rate in – Rate out + Rate of generation = Rate of accumulation

According to this the model, equations of the transient of all the species present in the system are as follows

$$\frac{d}{dt} C_{AA} = \frac{C_{AA_{in}} - C_{AA}}{V} F_{AA} - r_1 - r_2 \quad (4.5)$$

$$\frac{d}{dt} C_{ASA} = -\frac{C_{ASA}}{V} F_{AA} + r_1 \quad (4.6)$$

$$\frac{d}{dt} C_{HA} = -\frac{C_{HA}}{V} F_{AA} + r_1 + 2r_2 \quad (4.7)$$

$$\frac{d}{dt} C_{SA} = -\frac{C_{SA}}{V} F_{AA} - r_1 \quad (4.8)$$

$$\frac{d}{dt} C_W = -\frac{C_W}{V} F_{AA} - r_2 \quad (4.9)$$

$$\frac{d}{dt}V = F_{AA} \quad (4.10)$$

where

$V \equiv$  volume of the reactor

$F_{AA} \equiv$  flowrate of AA

Detailed derivation of the model equations can be found in Appendix A.

Using the  $\mathbf{C}_{\text{mod}}$  and  $\mathbf{A}$  (from the probe),  $\mathbf{E}$  can be estimated according to the equations given below

As

$$\mathbf{A} = \mathbf{C} \cdot \mathbf{E} \quad (4.11)$$

$$\Rightarrow \mathbf{E} = \mathbf{C}^{-1} \cdot \mathbf{A} \quad (4.12)$$

But since  $\mathbf{C}$  is not a square matrix it can not be inverted therefore the least-square solution to this would be

$$\mathbf{E}_{\text{est}} = \mathbf{C}^+ \cdot \mathbf{A} \quad (4.13)$$

where

$$\mathbf{C}^+ \equiv \text{pseudo inverse of } \mathbf{C} = \mathbf{C}^T \cdot [\mathbf{C}^T \cdot \mathbf{C}]^{-1}$$

$\mathbf{E}_{\text{est}} \equiv$  estimate of  $\mathbf{E}$

From this the mixture spectra can be estimated by

$$\mathbf{A}_{\text{est}} = \mathbf{C} \cdot \mathbf{E}_{\text{est}} \quad (4.14)$$

Graphically this procedure can be shown as follows.

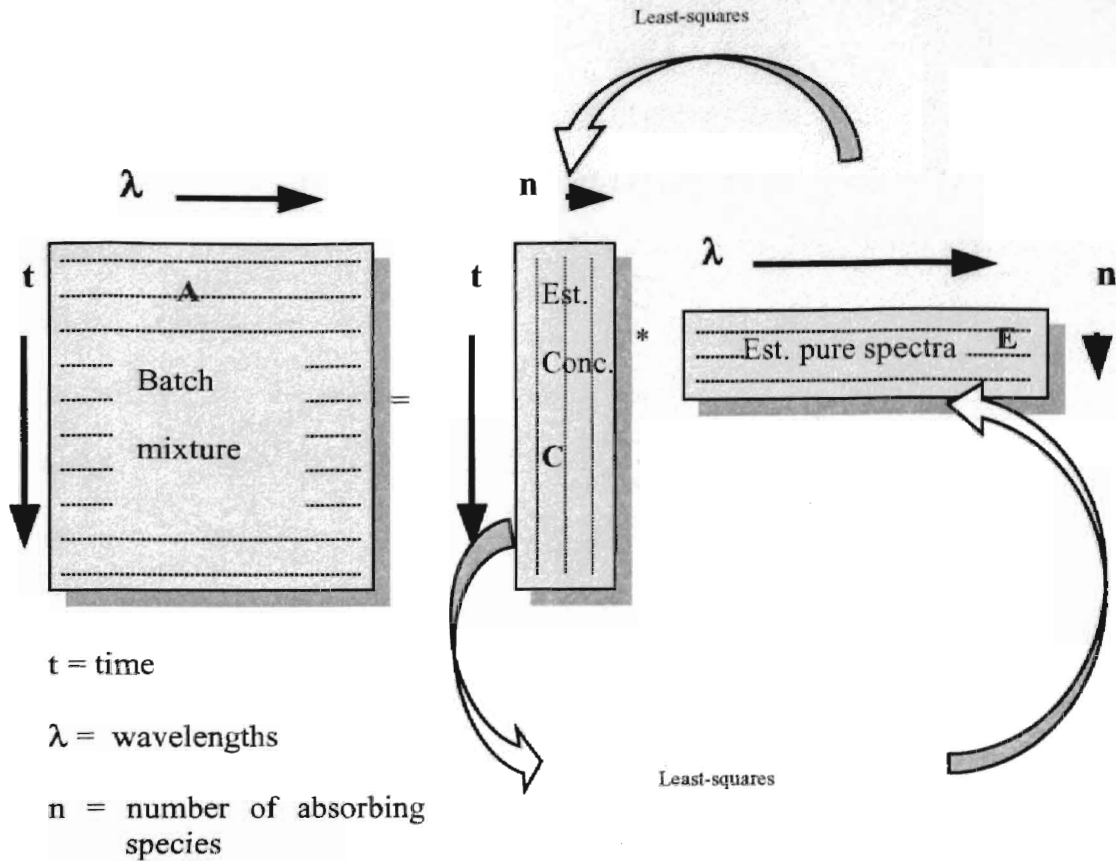


**Figure 4.2: Graphical representation of the least-square method**

If  $\mathbf{C}$  contains the true concentration profiles  $\mathbf{A}_{\text{est}}$  would be equal to  $\mathbf{A}_{\text{exp}}$ , but it is not so because the true concentration profiles are not known. So, the idea is to keep on regenerating  $\mathbf{C}_{\text{mod}}$  by changing the model parameters and reevaluating  $\mathbf{A}_{\text{est}}$  until  $\mathbf{A}_{\text{est}}$  matches  $\mathbf{A}_{\text{exp}}$ , when this is attained, the corresponding  $\mathbf{C}_{\text{mod}}$  would contain the true concentration profile, this shows that  $\mathbf{E}$  is not required to find the concentration profiles. Now to check if  $\mathbf{A}_{\text{est}}$  matches  $\mathbf{A}_{\text{exp}}$ , the sum of the squared difference between corresponding elements of  $\mathbf{A}_{\text{est}}$  and  $\mathbf{A}_{\text{exp}}$  is used and can be calculated by Equation 4.15.

$$J = \sum_{i=1}^m \sum_{j=1}^l (a_{ij} - a_{est\ ij})^2 \quad (4.15)$$

For  $\mathbf{A}_{est}$  and  $\mathbf{A}_{mod}$  to match perfectly  $J$  should be equal to zero, but due to signal noise a perfect match can never be attained. As signal noise is caused by un-measurable disturbances and cannot be accounted for in the kinetic model used to generate  $\mathbf{C}_{mod}$  which is used to generate  $\mathbf{A}_{est}$ . Therefore, the lowest possible value of  $J$  is used as an indication of a good match. To find the lowest value of  $J$  possible, a minimization routine is required. Since there is a non-linear relationship between  $J$  and model parameters a non-linear fitting routine was required. Once the best model coefficient have been found the estimated reference spectra is calculated by Equation 4.13.

In this case “fminsearch” a built-in MATLAB function, which is a Nelder-Mead type simplex search method (Lagarias, *et al.*, 1998), was used. “fminsearch” requires that the function to be minimized to accept single or multi variable input and returns a scalar output (further detail on “fminsearch” can be found in Appendix D). “fminsearch” was chosen because of its robustness compared to the other built-in minimization techniques available in MATLAB.

A function called “OF\_model” was created, (code is written in MATLAB script, shown in Appendix C), that takes model parameters as input, numerically solves model equations to generate concentration profiles, generates  $\mathbf{A}_{est}$ , access  $\mathbf{A}_{est}$  (stored on the hard drive), computes  $J$ , and returns the value of  $J$  as the output. “fminsearch” itself requires initial guesses of the parameters being optimized as input which it passes to the function being minimized.

After the parameter values are found, the kinetic model is used to generate concentration profiles. Then with a few simple algebraic equations (3.18 and 3.23), the reactant volume ( $V_{req}$ ) and time ( $t_{req}$ ) required to reach end-point can be obtained.

$$V_{req} = \frac{N_{AA_{req}}}{C_{AA_{in}}} \quad (4.9)$$

where

$$N_{AA_{req}} = N_{SA_o} + N_{W_o} - N_{AA_{added}} \quad (4.10)$$

$$\Rightarrow N_{AA_{req}} = C_{SA_o} V_o + C_{W_o} V_o - C_{AA_{in}} V_{added} \quad (4.11)$$

Similarly time required to complete the batch can be calculated as follows

After the final addition is made

$$F_{AA} = 0 \quad (4.12)$$

Then equation (3.18) becomes

$$\frac{d}{dt} C_{SA} = -r_1 \quad (4.13)$$

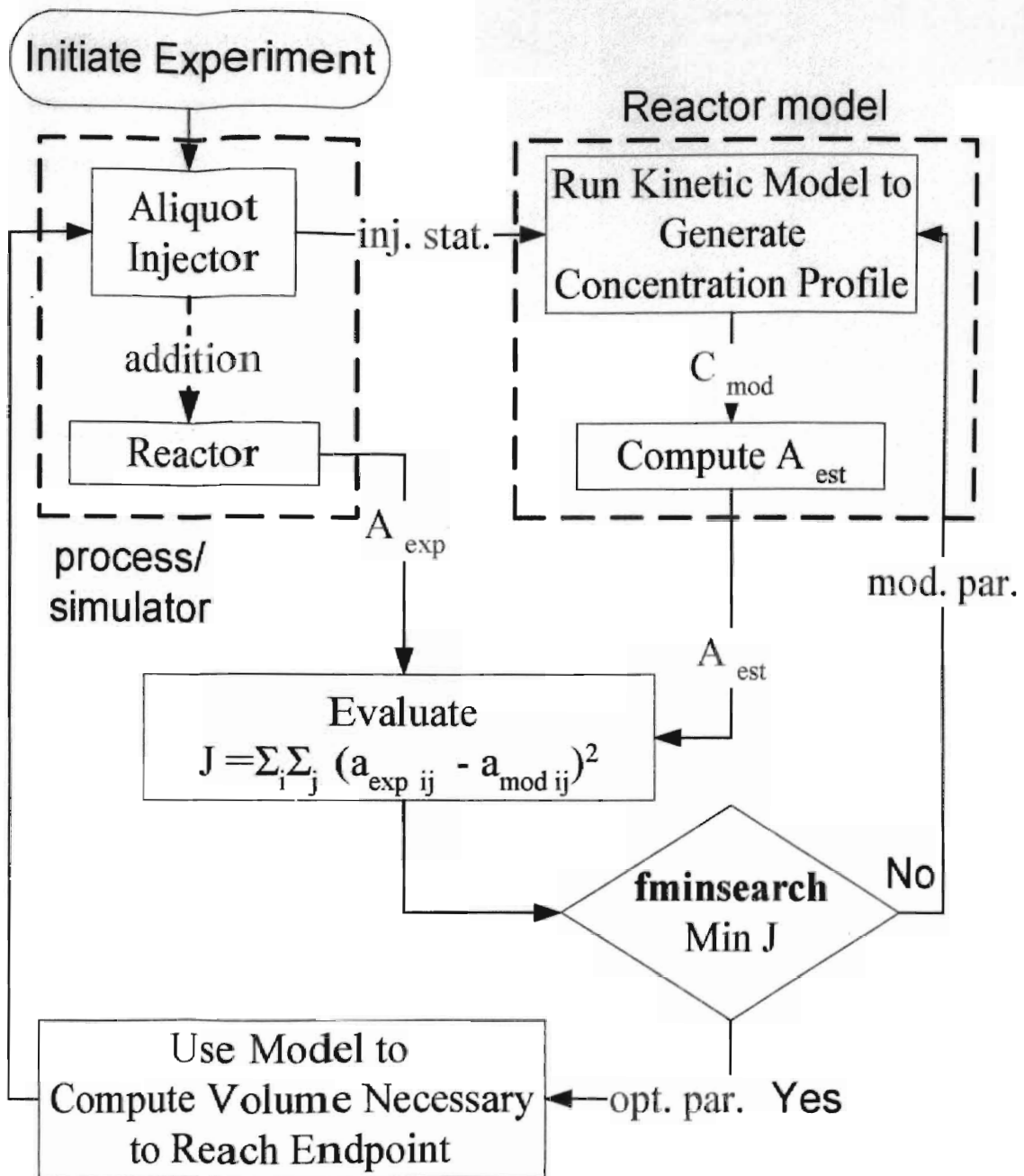
when solved for time it gives

$$t_{req} = \frac{1}{k_1} \int_{C_{SA}^*}^{tol\_C_{SA}} \frac{dC_{SA}}{C_{SA}(C_{SA_o} - C_{SA})} \quad (4.14)$$

where

$tol\_C_{SA} \equiv$  lowest tolerance of  $C_{SA} \approx 0$

$C_{SA}^* \equiv$  concentration of SA at time of evaluation



inj. stat.: injection statistics  
 mod. par.: model parameters  
 opt. par.: optimized model parameters  
 C<sub>mod</sub>: model generated concentration profile

Figure 4.3: Command flow diagram

The command flow diagram that graphically shows the technique described in this section as an on-line implementation tool can be seen in Figure 4.2. Which can be further explained as follows

Step 1: initiate experiment

Step 2: make first few additions

Step 3: collect spectral data and amount delivered

Step 4: use initial guesses to generate concentration profiles using the kinetic model

Step 5: generate  $\mathbf{A}_{est}$

Step 6: compare with  $\mathbf{A}_{exp}$

Step 7: if  $\mathbf{A}_{est}$  matches  $\mathbf{A}$ , goto Step 8, else goto Step 4

Step 8: uses kinetic model with optimized parameters to obtain  $V_{req}$  and make one final addition to the reactor.

Steps 4 through Step 7 are performed by “fminsearch”.



## 5. Simulations

### Process Simulator

For the process simulator the reactor was modeled as a perfectly mixed, stirred tank reactor containing only liquid phase, and all the reactions were assumed to be homogenous. The aliquot injection flowrate was assumed to be a step function, with quantity delivered to be exact. Instantaneous mixing of the aliquot was assumed, since in actual experiments amount added was small (about 1 mL per addition) and the rate of addition was slow (about 1 mL/min). Isothermal conditions are assumed as described earlier.

The simulations developed are based on the experimental system described above. Model equations are solved numerically to generate composition profiles and from them absorbance spectra is generated using Equation 3.4, where  $E$  used was obtained experimentally. Model parameters chosen to generate composition profile were such that the spectra obtained would be similar to experimental spectra. And, as the exact parameters are known, the algorithm under consideration may be tested.

To show versatility of the algorithm the rate law equation, the Reaction R1 was changed to

$$r_1 = k_{1f} C_{SA}^\alpha C_{AA}^\beta - k_{1r} C_{SA}^\gamma C_{AA}^\eta \quad (5.1)$$

where

$k_{1f}$   $\equiv$  kinetic constant for forward Rxn1

$k_{1r}$   $\equiv$  kinetic constant for reverse Rxn1

$\alpha, \beta, \gamma, \eta$   $\equiv$  order governing coefficients

This adds more dimensions to the problem, and shows the wide applicability of the algorithm as a generic tool for different chemical systems.

## 6. Results and Discussion

### Experimental Results

#### Experiment 1: 5\_01\_03

Two 1 ml additions of AA (Acetic Anhydride) separated by about thirty minutes were made at a flow rate of about 0.5 ml per minute to the reaction mixture. Four parameters,  $k_{1p}$ ,  $k_2$ ,  $C_{w0}$  (initial water concentration) and  $C_{SA0}$ , were used in the minimization routine with spectra shown in Figure 6.2(a) required by the ATR probe, placed inside the reactor, as the input to the algorithm.

Figure 6.1 shows the model generated concentration profiles, of all reacting species in the system, which was developed by using the model parameters found by the algorithm. A small amount of water is shown to be present in the beginning, but soon disappears as AA is added.

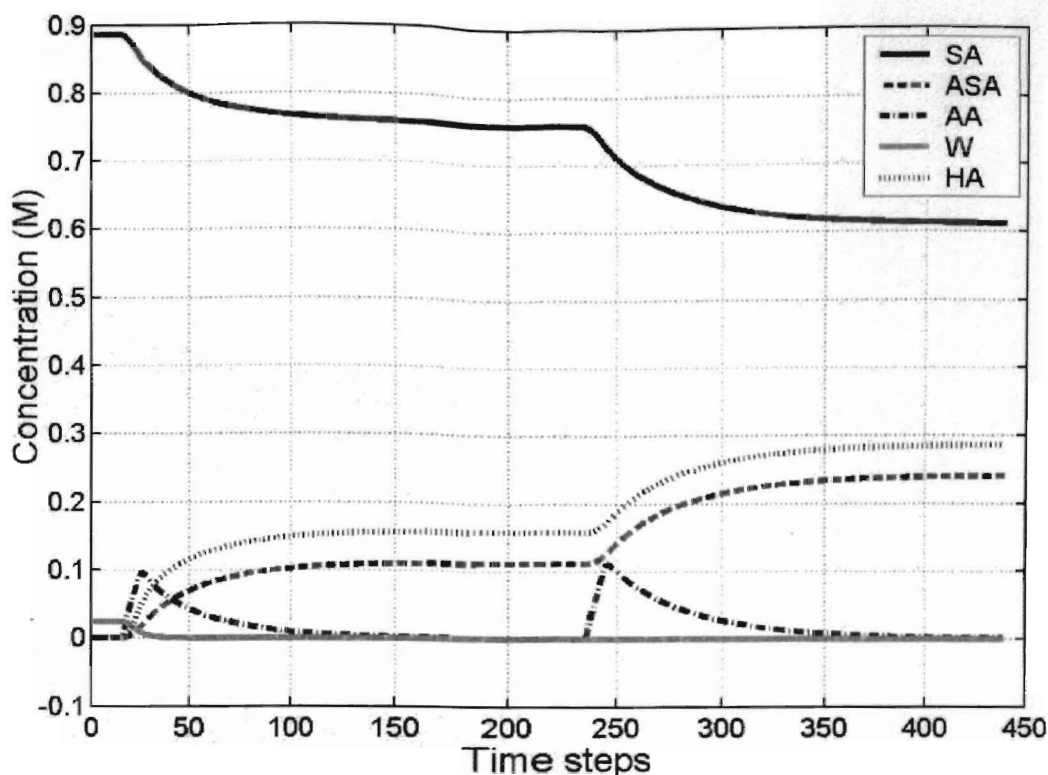


**Figure 6.1: Plot of Concentration Profiles as a function of time steps**

Figure 6.1 shows, (a) absorbance vs. time of spectra generated by the Algorithm, (b) absorbance vs. time of spectra obtained experimentally, (c) error of all absorbances at each point in time, between the corresponding values of  $A_{exp}$  and  $A_{est}$ , which reveals that the model generated spectra closely, resembles the experimentally obtained spectra

As can be seen in Figure 6.2 (c) error has the much higher value during the advent of every addition compared to when AA is not being added this behavior was seen with all experimental and simulation results. This may be because of the least squares type of minimization. As evident by the initial under shoot and then an over shoot and then a gradual decrease to almost zero of the error. Further research is needed to improve on the

minimization technique to ensure a better fit between  $A_{est}$  and  $A_{exp}$  during the interval of the addition.

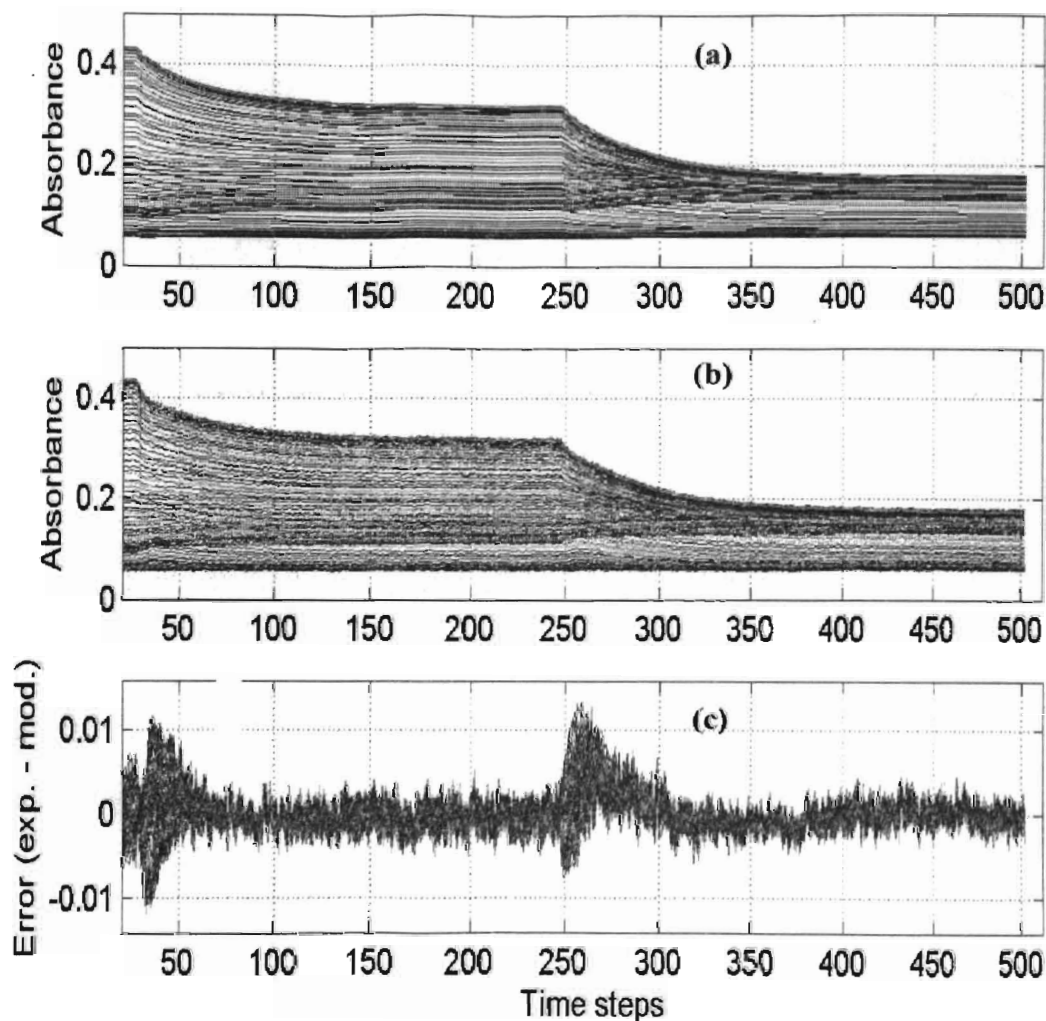


*Figure 6.2: Plots of Spectra for Exp. 5\_01\_03*

Although, there are region of mismatch between  $A_{exp}$  and  $A_{est}$ ,  $V_{req}$  came out to be 0.8163 ml which is 0.1776 ml more than prescribed by stoichiometry (0.6387 ml). The reason for this mismatch, although very small, is that the stoichiometric calculations were based

only on the 1:1 mole ratio of SA to AA and did not (and could not) account for the presence of water in the system. The amount of water cannot be determined by any non-invasive method available at the time of experiment. Evidence of the presence of water in the system is discussed later.

### Experiment 3

This experiment consisted of four separate batch experiments which were setup identically, each experiment was named for the date it was performed on, only difference being was that two batches (Experiments 9\_3\_02 and 9\_6\_02) had small amounts of water added to them and not to the other two (Experiments 9\_13\_02 and 9\_27\_02). In this experiment, four parameters,  $k_{1f}$ ,  $k_{1r}$  (kinetic constant for the reverse of Reaction R1),  $k_2$ , and  $C_{w0}$  (initial water concentration), were adjusted in the minimization routine, and the rest were set constant at the known values. Although it is known that SA and AA react irreversibly at the temperature the experiments were being conducted,  $k_{1r}$  was used during minimization to see if the Algorithm would be able to determine this fact. This experiment was designed to test the accuracy of the Algorithm's in predicting the amount of water present in the system, that is the reason for the not using initial concentration of SA as one of the parameters being adjusted in the minimization step.

Table 6.9 shows the values of the kinetic constant determined by the Algorithm and it shows that for all four experiments  $k_{1r}$  had values very close to being zero. Values of  $k_{1r}$  determined by the Algorithm were all numerically similar to each other averaging at 0.4375 with a standard deviation of 0.1107. The similarities in the values of kinetic

constant determined by the Algorithm for different experiments suggest high robustness of this Algorithm.

*Table 6.1: Experimental results, kinetic constants*

Experiment	k1_f [L/(mol*min)]	k1_r [L/(mol*min)]	k2 [L/(mol*min)]
9_3_02	0.3828	0.0000	91.2563
9_6_02	0.4041	0.0001	41.0756
9_13_02	0.3617	0.0000	0.2220
9_27_02	0.6015	0.0000	0.0000
Average	0.4375	0.0000	33.1385
Std. Dev.	0.1107	0.0001	43.2910

Values for  $k_2$  for experiments with no water added came out similar to each other but not for the experiment in which there was water added. The reason for this mismatch may be because of experimental error specifically the amount of water added in Experiment 9\_6\_02, since there is difference between, theoretical initial concentration of water and the initial concentration determined by the algorithm (Table 6.2), and between the theoretical  $V_{req}$  and Algorithm determined  $V_{req}$  (Table 6.3).

**Table 6.2: Experimental results, initial Conc. of Water**

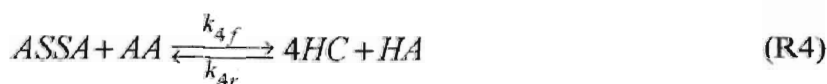
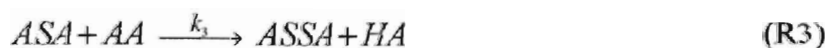
Experiment	CW <sub>0</sub> [M]	CW <sub>0</sub> theo. [M]	% diff
9 3 02	0.3062	0.3104	1.3623
9 6 02	0.4950	0.3104	45.8406
9 13 02	0.0001	0.0000	200.0000
9 27 02	0.0000	0.0000	#DIV/0!

**Table 6.3: Experimental results, V<sub>req</sub>**

Experiment	V <sub>req.</sub> theo. [mL]	V <sub>req</sub> [mL]	% diff
9 3 02	0.9547	0.9493	0.5672
9 6 02	0.9747	1.2857	27.5173
9 13 02	0.3813	0.3814	0.0184
9 27 02	0.0193	0.0194	0.5168

#### Experiment 4

In this experiment different possible side reactions, suggested by Dr. Gemperline, were included in the kinetic model used by the Algorithm, and are given below.



where

ASSA ≡ Acetylsalicylic Salicylic Acid

HC ≡ Hydroxy Coumarin



The Algorithm was used on previously collected spectra, with kinetic parameters for these reactions included as parameters for minimization. The Algorithm determined values for the kinetic parameters for the above given reactions were always very close to zero suggesting the non occurrence of Reaction R3, R4, and R5.

### Constant Ratio

The initial concentration of neither of the two reactants is required to find the correct  $V_{req}$  value. Either one of the parameters ( $C_{SA0}$  or  $C_{AAin}$ ) can be arbitrarily set to a constant value, and the other could be searched for by the minimization routine. But, this method only yields the correct  $V_{req}$  value, not necessarily the correct values of the other parameters as they are related to the initial concentration of the reactants.

**Table 6.4: Constant Ratio Results**

RUN #	CSA0 [M]	CAAin [M]	Cw0 [M]	Vreq [mL]
1	<b>1.0000</b>	7.7498	0.0267	0.8163
2	<b>0.8830</b>	6.8523	0.0237	0.8163
3	1.3652	<b>10.5800</b>	0.0365	0.8163

Bold represent fixed values

It can be seen in the fourth column of Table 6.4 that the ratio  $C_{SA0} / C_{AAin}$  and  $V_{req}$  comes out same for different constant values of  $C_{SA0}$  or  $C_{AAin}$ . Same behavior is observed while using spectra from other sets of experiments and also from using simulated spectra.

In order to further explain this find, a surface map of the objective function value (J) was plotted as a function of  $k_1$  and  $C_{AAin}$  as shown in Figure 6.3, different layers of surfaces represent different values of  $C_{SA0}$ . Although there are more than three parameters that are

unknown during actual experiments, only these three  $k_1$ ,  $C_{SA0}$ , and  $C_{AAin}$  were chosen as changes in the value of these parameters are the most dominating cause of change in the objective function value. And, also because it is difficult to graphically represent systems with more than three variables.

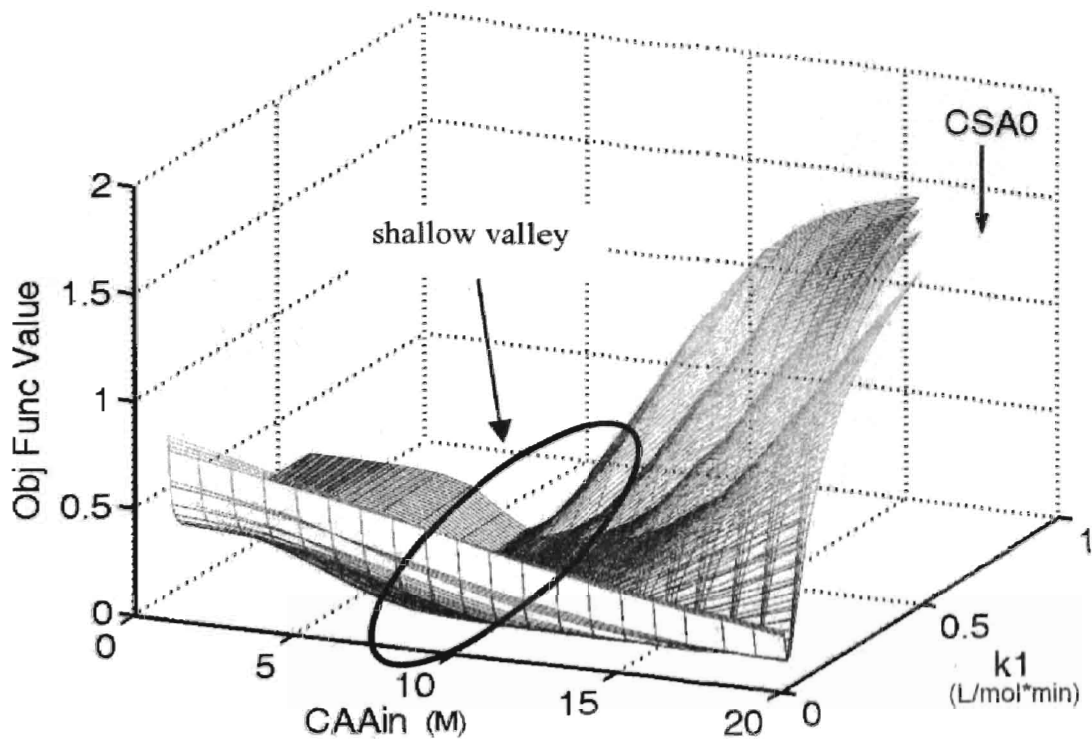


**Figure 6.3: Surface Plot 1 of the Objective Function Value ( $J$ )**

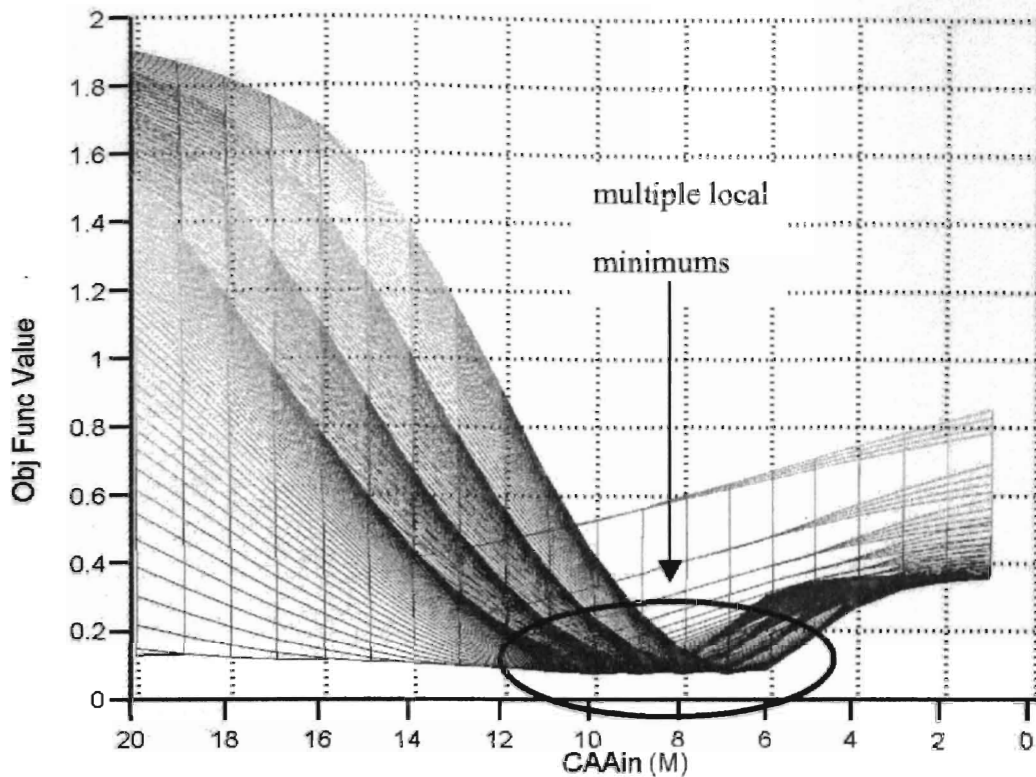


**Figure 6.4: Surface Plot 2 of the Objective Function Value ( $J$ )**

Figure 6.4 shows the same thing as shown in Figure 6.3, only the viewing angle is different, for ease of explanation. Figures 6.3 and 6.4 show that in every layer of the surface map there are shallow valleys with closely located minimums, which indicates that the objective function value can be same for many different values of the parameters.

## Presence of Water

Figure 6.5 shows that there is a 15.6 % greater change in the absorbance caused by the second addition of AA compared to the first addition.

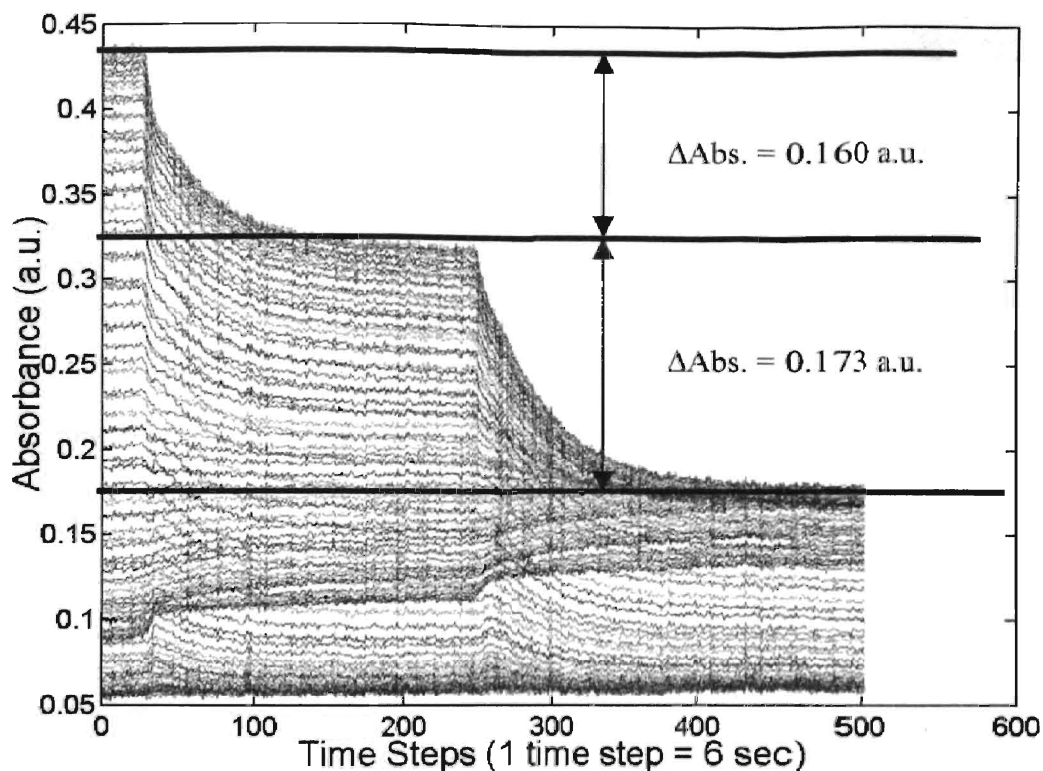


*Figure 6.5: Zoomed in view of Figure 6.2 (a), Exp. 5\_01\_03*

Since, SA is the only absorbing species that is also being consumed and the amount of AA added in the first addition is the same as the amount added in the second addition, a drop in absorbance in the first step being less than the drop in the second step indicates that some of the AA added in the first addition reacted with some species other than SA.

Although, this species could be anything that reacts with AA under these conditions, the most likely candidate is water. This deduction is based on the fact that powdered SA as well as the solvent acetonitrile can both absorb water from the atmosphere, and the humidity level are usually high in the place where the experiments being reported here took place. Another source of the presence of water is the apparatus cleaning procedure. Although great care was taken to reduce the chances of water being present it does not guarantee complete absence of water in the system.

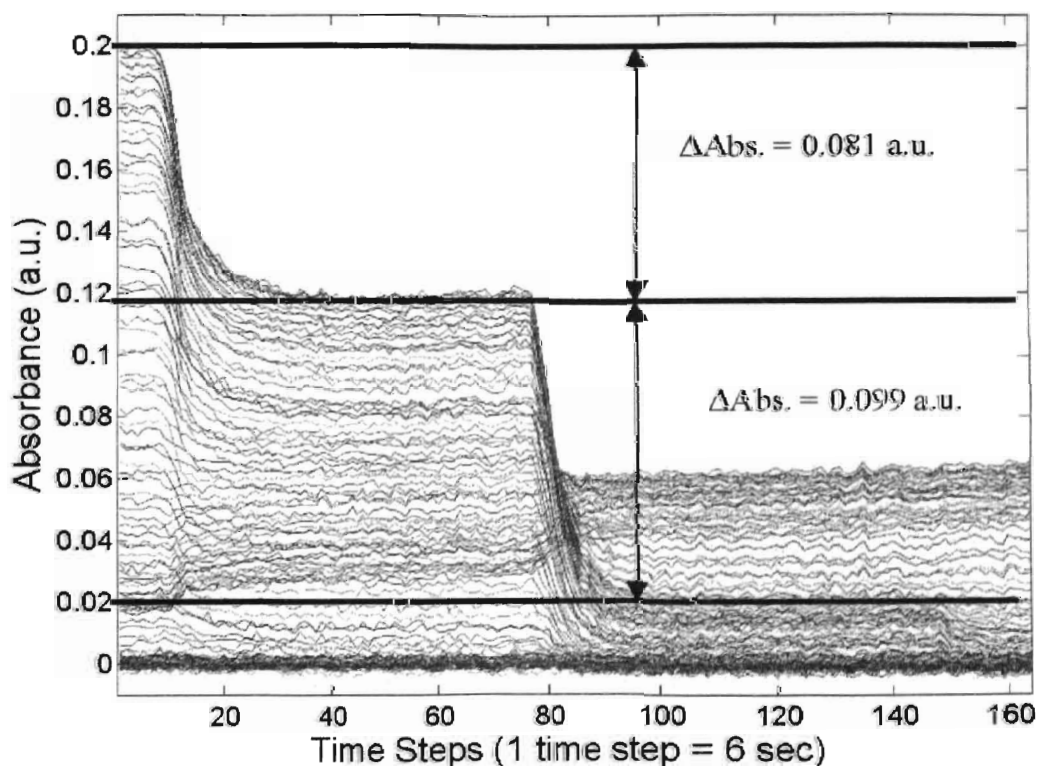


*Figure 6.6: Plot of Absorbance vs. Time Steps for Exp. 9\_27\_02*

Figure 6.6 also indicates towards the same deduction only in this case there is a 40% greater change in the absorbance caused by the second addition of AA compared to the

first addition indication a larger amount of water present compared to that present in the system for Exp. 5\_01\_03.

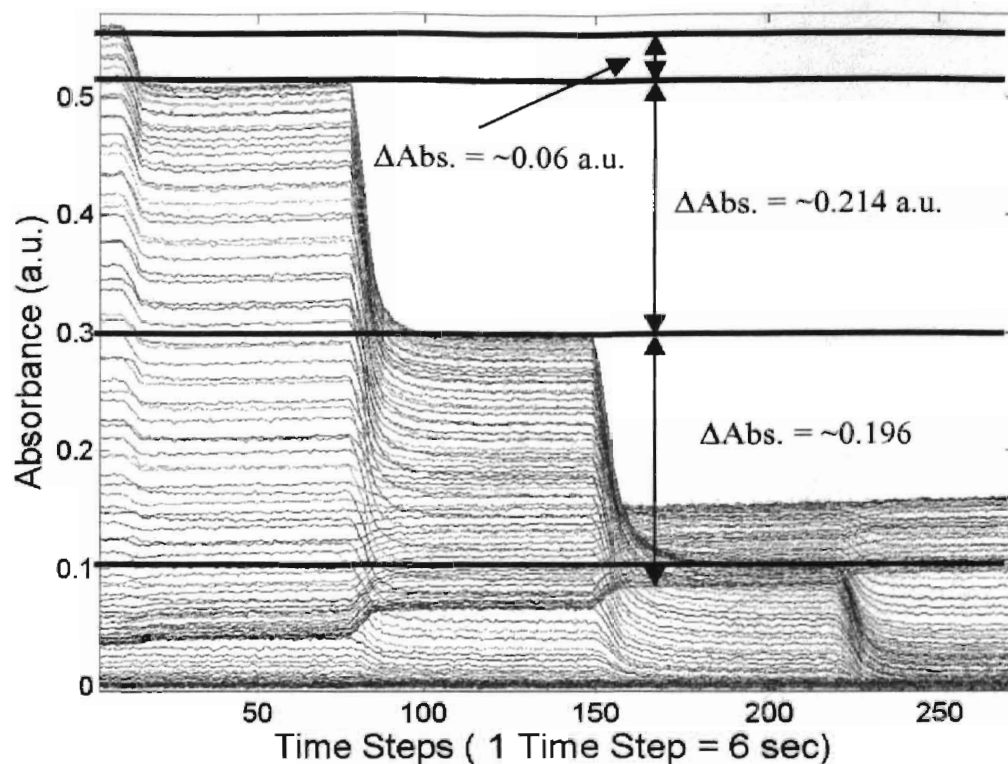


**Figure 6.7: Plot of Absorbance vs. Time Steps for Exp. 9\_6\_02**

Figure 6.7 shows the spectra of an experiment in which three additions of AA were made. In this experiment a small amount (10% mole ratio of AA) of was added. It can be seen that the change in absorbance in the first step is much smaller (214% smaller) than the change in the second step as was expected because the presence on larger amount of water compared to the previous two experiment. The change in absorbance in the second step match the change in the third step (only a difference of 3%), indicating that the contaminant (Water) was almost all consumed by AA in the first addition. All these

results validate the hypothesis of the presence of water in the system a reacting contaminant. The results shown in this section are also the reason for using spectra obtained after two or more additions were made to the batch, since there is information about two species in the system. Using information after two additions seemed to insure that enough information is acquired to accurately characterize a batch. Only one addition would have provided enough if all the species in the system absorbed uniquely in the UV/Vis wavelength range. Further research is needed to develop a technique, which would determine when enough spectral data has been collected to guarantee the complete characterization of the batch.

### **Experimental Difficulties**

The main difficulty faced was in identifying the exact cause of absorbance drift. To rule out reaction as the cause of the absorbance drift, an experiment was designed (Exp. 1\_10\_03), in which a reaction did not take place. The reactor was charged with only acetonitrile (ACN, solvent of choice for all batches), and then two additions of SA in dissolved in the ACN and two additions of only ACN were made the rest of the procedure for startup was the same as that of other previous reactionary experiments. The second pair of additions was made to rule out the non instantaneous mixing hypothesis.

Figure 6.8 shows the absorbance vs. time step plot of spectra obtained during this experiment. As expected, since SA is an UV/Vis absorbing species, a two step rise in absorbance is observed caused by the two additions of SA. Then a two step drop is observed which is caused by the dilution of the solution due to the two additions of the acetonitrile. The initial instantaneous rise in absorbance due to the two SA additions and

initial instantaneous drop in absorbance due to the two additions, also validate the instantaneous mixing assumption, made during the development of the model. One point to be noted here is the absence of drift before any additions were made, meaning that the cause of drift is in hidden the presence of SA in the system, supporting the hypothesis made earlier that drift is caused by the adsorbance of SA to the surface of the UV/Vis ATR probe crystal.

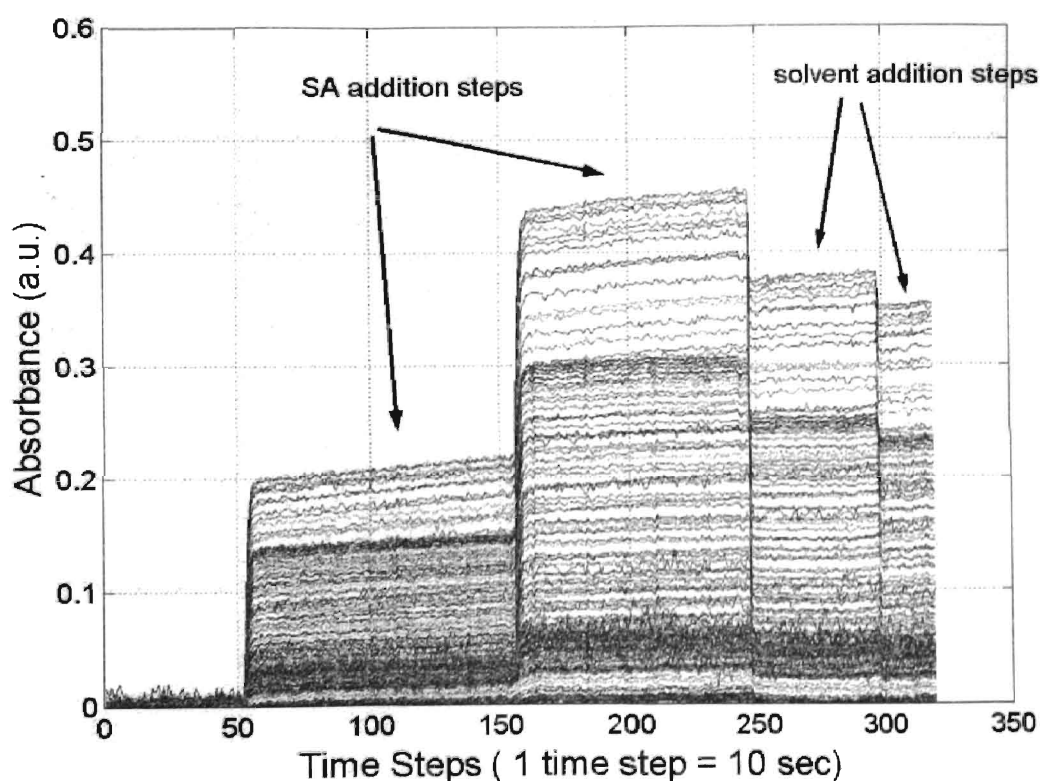


**Figure 6.8: Plot of Absorbance vs. Time Steps for Exp. 1\_10\_03**

Figure 6.9 shows a zoomed in view of the spectra caused by the two SA additions. The black lines drawn over the first two steps of spectra have the same slope, which matches the rate of increase of absorbance, indicating the drift in the first two steps follows the same mechanism.



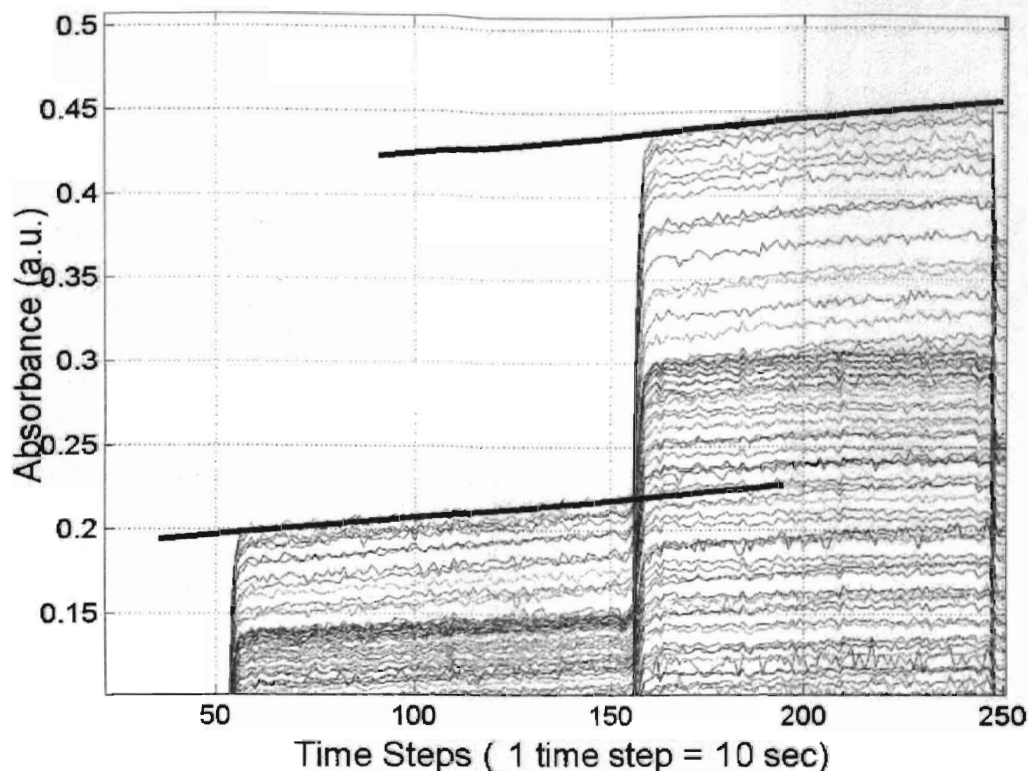


***Figure 6.9: Plot of Absorbance vs. Time Steps for Exp. 1\_10\_03***

Figure 6.10 shows a zoomed in view of the spectra caused by the two ACN additions. The grey lines drawn over the second two steps of the plot of spectra do not have exactly the same slope the slope of the line over the last step is very slightly smaller than the slope of the previous step. Indicating the drift in the second two steps may not follow the same mechanism. The two red lines also do not have the same slope as that of the slope of the black line, showing that the rate of change in absorbance although similar are not the same for the first two steps and that of the second two step.

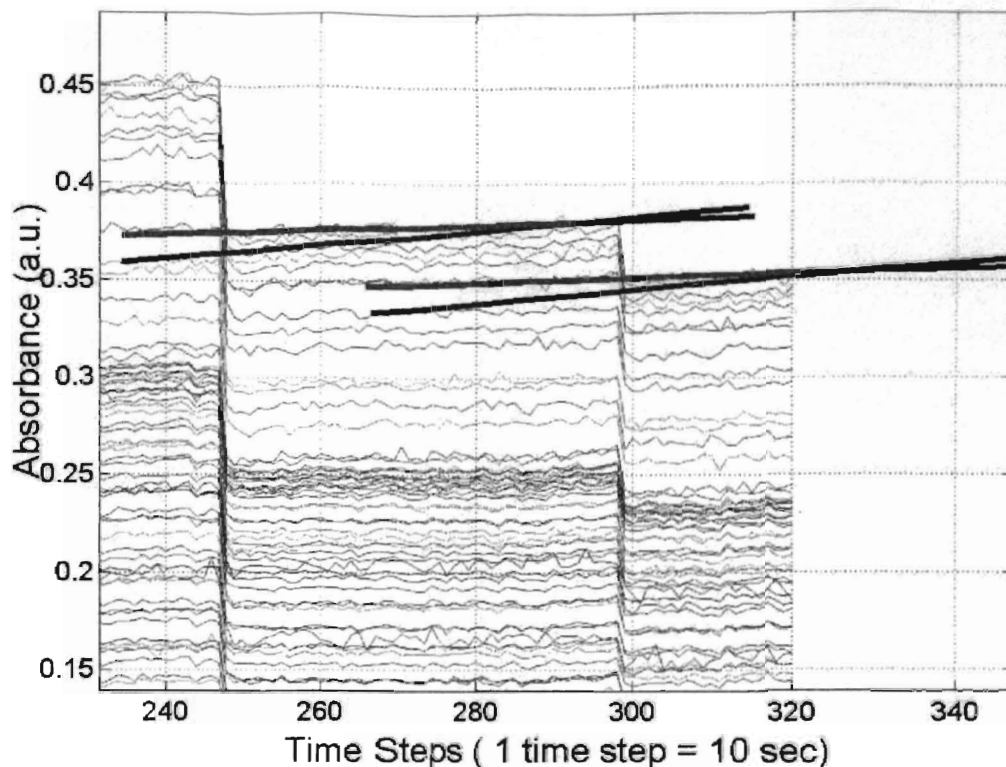


**Figure 6.10: Plot of Absorbance vs. Time Steps for Exp.1\_10\_03**

This indicates that the mechanism of drift caused by the addition of SA is not the same as that caused by ACN addition. It can be seen that the absorbance was still changing when the ACN additions was made indicating that the drift seen in the last two steps may be due to continuing effect of SA adsorbing to the crystal. Since the bulk concentration has dropped due to the addition of the solvent, the rate of change has decreased from that in the first two steps. Another experiment was conducted in which only one addition of SA was made to the solvent and the spectra was observed for a substantial amount of time (about three hours) to examine if the rate on change in absorbance ever diminishes. It took a little more than 2 hours for the drift to disappear, indicating that drift follows a very slow mechanism. Further research is required to determine the exact cause of drift

and to find ways of removing it or modeling it, and also to observe sensitivity of the Algorithm, in predicting the correct amount of volume required to complete the batch, to the presence of drift in spectra.

The other difficulty faced was that no experimental method was available to validate the findings of the Algorithm. A non invasive method for making concentration measurements is required, which does not require taking samples from the batch because since it is very difficult guarantee that the reaction can be quenched without losing any information about the concentration of all the species in the system.

### **Simulation Results**

For simulation experiments, spectra (**A**) was generated by using Equation 4.3 with true species spectra (**E**) represented by that obtained experimentally and concentration profile (**C**) generated by the kinetic model with known parameter values. Only **A** was used as the input to the algorithm described above. **E** or **C**, which were used to create **A**, were treated as unknowns since they are not known in actual experiments.

#### **Simulation 1**

This simulation experiment was designed to show that the technique described in this thesis can be used to determine the volume of the reactant and the time required to reach the end-point while the reaction rate law, reaction rate constants, reaction order and initial concentration of the reactants are not known.

Seven out of the ten possible kinetic model parameters were chosen for minimization, the rest were set constant at the known values. The chosen parameters were  $k_{1f}$ ,  $k_{1r}$ ,  $C_{SA0}$  (initial SA concentration),  $\alpha$ ,  $\beta$ ,  $\gamma$ , and  $\eta$ .

As shown in Table 6.5, all parameter values, except values for  $\gamma$  and  $\eta$ , exactly match the known values.  $\gamma$  and  $\eta$  values do not match exactly because they represent excess degree of freedom. Although they do not match the known values;  $V_{req}$  is always (considering similar simulation results) correct.

**Table 6.5: Parameter values for Simulation 1**

Parameter	Known Value	Algorithm Determined
$k_{1f}$ [L / (mol * min)]	0.1	0.1000
$k_{1r}$ [L / (mol * min)]	0.001	0.0010
$k_2$ [L / (mol * min)]	0	Set Const.
$C_{wo}$ [M]	0	Set Const.
$C_{AAin}$ [M]	10	Set Const.
$C_{SA0}$ [M]	2	2.0000
$\alpha$ [unit less]	1	1.0000
$\beta$ [unit less]	1	1.0000
$\gamma$ [unit less]	1	1.0326
$\eta$ [unit less]	1	0.9674
$V_{req}$ [mL]	2.9967	2.9967
$t_{req}$ [min]	unknown	39.9622

Noise was generated by using a built in function in MATLAB called “rand(m,n)”, which can be used to generate an m-by-n matrix of random numbers with uniform distribution of 0.01 centered at 0. This matrix containing random numbers is simply added to the spectra matrix obtained in Simulation 1 to represent experimentally obtained spectra. The same experiment as described above was repeated to see the sensitivity of the Algorithm to noise. Only an error of +1.1 % between  $V_{req}$  known and  $V_{req}$  determined by

the Algorithm was seen. This shows applicability of the Algorithm, as a tool to determine volume required to reach end-point in actual experiments.

To further evaluate the sensitivity of the Algorithm to noise, similar experiments were performed, with different sets of simulated spectra, which indicated the magnitude of percent error, between  $V_{req}$  known and  $V_{req}$  determined by the Algorithm was, depended on the level of noise, the higher the noise level the higher was the error. And, the error at some instances came out negative and at some came out positive, which was an expected outcome, since when the sample size is not infinite, signal noise is naturally biased and if averaged over a finite sample size does not yield exactly zero.

## **Simulation 2**

In the second simulation, four parameters,  $k_{1p}$ ,  $k_2$ ,  $C_{w_0}$  (initial water concentration) and  $C_{SA_0}$ , were adjusted in the minimization routine. The rest were set constant at the known values. This simulation was mainly designed to show that the technique can be used to determine the volume of the reactant and the time required to reach the endpoint while a side reaction is occurring that consumes one of the reactants. Also, rate constants and initial concentration of one of the reactants and the initial concentration of the impurity are unknown.

**Table 6.6: Parameter values for Simulation 2**

Parameter	Known Value	Algorithm Determined
$k_{1f}$ [L / (mol * min)]	0.1	0.1000
$k_{1r}$ [L / (mol * min)]	0	Set Const.
$k_2$ [L / (mol * min)]	1	1.0000
$C_{wo}$ [M]	0.25	0.2500
$C_{AAin}$ [M]	10	Set Const.
$C_{SA0}$ [M]	2	2.0000
$\alpha$ [unit less]	1	Set Const.
$\beta$ [unit less]	1	Set Const.
$\gamma$ [unit less]	1	Set Const.
$\eta$ [unit less]	1	Set Const.
$V_{req}$ [mL]	3.5	3.5000
$t_{req}$ [min]	unknown	37.4208

In this simulation water was present as an impurity that reacts with AA at a rate that is ten times faster than the rate of reaction between AA and SA. As can be seen in Table 2 below all parameter values found by the minimization routine exactly match the known values as well as  $V_{req}$ .

### Simulation 3

This simulation was designed to show the applicability of the Algorithm in the presence of model mismatch. Spectra was generated by using the concentration profiles that were generated by the kinetic model in which kinetic constant value for R1 varied with change in volume. The following equation represents kinetic constant value.

$$k_{1f} = k_{1finitial} \frac{V_{initial}}{V} \quad (6.1)$$

where

$k_{1finitial}$  = initial value of  $k_{1f}$

$V_{initial}$  = initial volume

According to Equation 6.1 that the kinetic constant value decreases as the volume increases, this may be caused by the density decrease of the reaction mixture. Although the main reason behind the choice of this mechanism was its simplicity and ease of implementation to simulate variations in reaction rate constants, which in actual experiments may be caused due to slight variations in operating condition such as variation in temperature, pressure and etc. This variation in the kinetic constant was not accounted for the in the model equations used by the Algorithm to create model mismatch.

Four parameters,  $k_{1f}$ ,  $k_2$ ,  $C_{w_0}$  (initial water concentration) and  $C_{SA_0}$ , were adjusted in the minimization routine. There was also a difference in recipe management. After first simulated addition the spectra generated was fed to the Algorithm and  $V_{req}$  was obtained and then 50% of the  $V_{req}$  was simulated as the second addition to the reactor and spectra only from the second addition was fed to the Algorithm, for subsequent additions, instead of simulating adding 50% of the  $V_{req}$ , 75% and 90% of  $V_{req}$  were added, since it was assumed (shown later to be true) that the accuracy in the determination of  $V_{req}$  after every addition improve would due to the fact that  $V_{req}$  became smaller after every addition made. According to the above made assumption, the determination of  $V_{req}$  after the first addition would be the least accurate therefore to reduce the possibility of adding excess

amount of AA only 50% percent of the  $V_{req}$  prescribed by the Algorithm was added, and as the accuracy increases the confidence level increases and larger percentage of  $V_{req}$  are added in the later steps. Although, Algorithm determined parameter values, other than of  $V_{req}$ , do not accurately match the known values as shown in Table 6.4-6.7,  $V_{req}$  values do match more accurately as shown in Table 6.3. Determining the correct  $V_{req}$  value is of more importance in this project than to determine other parameter values. Furthermore Table 6.3 shows that the percent error in  $V_{req}$  reduced with every addition since  $k_{1r}$  was determined individually after every addition and since the volume added became smaller.

This indicates that even with a model mismatch, such as variation in the kinetic constant which may be caused by indeterminable reasons, this Algorithm with model re-parameterization after every addition can be confidently used to determine  $V_{req}$ . In the case of this simulation it was known that the variation in the kinetic constant occurs in every addition therefore re-parameterization was done after every addition, for actual experiments in which the variation may be undetectable re-parameterization can be done at short intervals of time to maintain a good match between the model and the process.



**Table 6.7:  $V_{req}$  values for Simulation 3**

	$V_{req}$ , Algo. det. [mL]	$V_{req}$ , actual [mL]	% error
1st addition	3.5881	3.5000	2.52
2nd addition	2.2582	2.4000	-5.91
3rd addition	0.6672	0.6942	-3.89
4th addition	0.0170	0.0174	-2.30

**Table 6.8:  $k_2$  values for Simulation 3**

	$k_2$ , Algo. det. [L/(mol *min)]	$k_2$ , actual [L/(mol *min)]	% error
1st addition	1.7187	1.0000	71.87
2nd addition	0.7800	1.0000	-22.00
3rd addition	1.5124	1.0000	51.24
4th addition	1.4940	1.0000	49.40

**Table 6.9:  $k_{1f}$  values for Simulation 3**

	$k_{1f}$ , Algo. det. [L/(mol *min)]	$k_{1f}$ , actual [L/(mol *min)]	% error
1st addition	0.1048	0.0975	-7.49
2nd addition	0.0922	0.0952	3.19
3rd addition	0.0879	0.0909	3.33
4th addition	0.0698	0.0741	5.74

**Table 6.10:  $C_{wo}$  values for Simulation 3**

	Cwo, Algo. det. [M]	Cwo, actual [M]	% error
1st addition	0.1007	0.2500	-59.72
2nd addition	0.1515	0.0309	390.29
3rd addition	0.0000	0.0000	#DM/0!
4th addition	0.0000	0.0000	#DM/0!

**Table 6.11:  $C_{SAo}$  values for Simulation 3**

	CSAo, Algo. det. [M]	CSAo, actual [M]	% error
1st addition	1.7277	2.0000	-13.62
2nd addition	1.7776	1.5090	17.80
3rd addition	1.1867	0.9400	26.24
4th addition	0.3488	0.2572	35.61

All the numerical experiments done with simulated spectra were repeated with using only absorbance as function of time data at only two wavelengths, one from the range that SA absorbs and one from the range that ASA absorbs. The two wavelengths chosen had the maximum change in the magnitude of absorbance at each addition, to ensure high signal to noise ratio. The results obtained by using only two wavelength data as the input to the Algorithm were the same as those obtained previously, but the Algorithm convergence time was much faster (10 times faster).

## 7. Future Directions

This technique can be used as an off-normal operation identifier, by using batch-to-batch data and plotting and comparing parameter values with the value obtained from previous batches. If the parameter values determined by the Algorithm vary by a great margin from the general trend found in the previous batches parameter values then off-normal behavior can be suspected.

Versatility of this technique can be increased by, adding code that would automatically generate kinetic model based on the kinetic information provided by the user, by including energy balance in the model so that thermal data could be matched in addition to spectra, which would provide further assurance in the solution found by the Algorithm, and by adding steady state identifier type algorithm to identify when enough information has been collected to give a reasonable solution.

## 8. Conclusions and Recommendations

By monitoring the reactor's time-dependent spectroscopic response, after a few small additions of one of the reacting reagents, the kinetic model can be adjusted online. The adjusted model can be then used to find the stoichiometric amount needed to complete the batch. Large reagent additions can then be confidently made to reach the endpoint rapidly, thereby shortening the batch time, minimizing reagent consumption, improving yield, and reducing impurities in finished batches.

There are a few issues of concern and limitations to this technique.

- Needed two additions to produce correct results.
- Results were highly dependent on the amount of noise in the spectral data.
- Results were highly dependent on the initial guesses used for the input to the Algorithm.

The use of the technique described in this thesis has not been experimentally, definitely, shown to be an online tool since we cannot independently confirm the presence of water and we do not yet have a technique to test for excess AA after the final addition has been made. However simulation experiments strongly support the concept and the Algorithms, and experiments provide no contradiction.

There appears to be several issues that need to be solved prior to on-line industrial application of this technique.

- Drift in sensor.
- Computational speed of the Algorithm.
- Identifying when sufficient data is captured to generate confidence in model parameters.
- A universal strategy for tempering additions as the most recent data improves the model.
- Time coordination of spectra and flow data.
- Algorithm development should include a thermal model.
- Sensitivity of the probe to temperature fluctuations.
- A method is needed to make independent concentration measurements to validate Algorithm findings.
- Development of a problem specific minimization technique.
- Using information from wavelength range other than UV/Vis should also be analyzed, this may give information about the species that do not absorb in the UV/Vis range.

## References

1. Abel, O., A. Helbig, W. Marquart, H. Zwick, and T. Daszkowski, "Productivity Optimization of an Industrial Semi-batch Polymerization Reactor under Safety Constraints", *J. Proc. Cont.*, **10**(4), 351-362 (2000)
2. Bezemer, E., S. C. Rutan, "Multivariate Curve Resolution with Non-Linear Fitting of Kinetic Profiles", *Chemometrics and Intelligent Laboratory Systems*, **59**, 19-31, (2001)
3. Bijlsma, S., D.J. Louwse (Ad), W. Windig, A. K. Smilde, "Rapid Estimation of Rate Constants Using On-line SW\_NIR and Trilinear Models"
4. Bijlsma, S., H. F. M. Boelens, H. C. J. Hoefsloot, A. K. Smilde, "Estimating Reaction Rate Constants: Comparison between traditional Curve Fitting and Curve Resolution", *Analytica Chimica Acta*, **419**, 197-207, (2000)
5. Bonvin D., B. Srinivasan and D. Ruppen, "Dynamic Optimization in the Batch Chemical Industry", *AIChE Symposium Series* No. 326, Vol. **98**, 255-273 (2002)
6. Bonvin, D., "Optimal Operation of Batch Reactors: A personal view," *J. Proc. Cont.*, **8**(5-6), 355-368, (1998)
7. Burns, D. A., E. W. Ciurczak. "Handbook of Near-Infrared Analysis", Marcel Dekker, New York, (1992)
8. Choi, J. Y., R. R. Rhinehart, and P. K. Mercure, Optimization of a Batch Polymerization Reactor, in *World Batch Forum*, Houston, TX, Apr., (1997)
9. Dhir, S., K. J. Morrow, Jr., R. R. Rhinehart, and T. Wiesner "Dynamic Optimization of Hybridoma Growth in a Fed-Batch Bioreactor", *Biotech. Bioeng.*, **67**(2), (2000)

10. Dong, D., T. J. McAvoy, and E. Zafiriou, "Batch-to-Batch Optimization using Neural Networks", *Ind. Eng. Chem. Res.*, **35**, 2269-2276 (1996)
11. Eaton, J. W. and J. B. Rawlings, "Feedback Control of Nonlinear Process using On-line Optimization Techniques", *Comput. Chem. Eng.*, **14**, 469-479, (1990).
12. Gemperline, P. J., M. Zhu, E. Cash, and D. S. Walker, "Chemometric Characterization of Batch Reactions", *ISA transactions*, **38**, 211-216 (1999).
13. Iyer, M. S.; T. F. Wiesner, and R. R Rhinehart, "Dynamic Re-optimization of a Fed-Batch Fermentor", *Biotech. and Bioeng.*, **63**, 10-21, (1999)
14. Johnson, A., "The control of fed-batch fermentation processes, a survey", *Automatica*, **23**, 691-705 (1987).
15. Lagarias, J.C., J. A. Reeds, M. H. Wright, and P. E. Wright, "Convergence Properties of the Nelder-Mead Simplex Method in Low Dimensions," *SIAM Journal of Optimization*, Vol. **9** Number 1, pp.112-147, 1998.
16. Lawton, W. H., E.A. Sylvestre, "Self Modeling Curve Resolution", *Technometrics*, **13** 617-663 (1971)
17. Le Lann, M. V., M. Cabassud, and G. Casamatta, Modeling, Optimization, and Control of Batch Chemical Reactors in Fine Chemical Production, in *IFAC DYCOPS-5*, 751-760, Corfu, Greece (1998)
18. Love, J., "Trends and Issues in Batch Control", *The Chem. Engineer*, Apr. (1988)
19. Quinn, A. C., P. J. Gemperline, B. Baker, M. Zhu, and D. S. Walker, "Fiber-optic UV/visible Composition Monitoring for Process Control of Batch Reactions", *Chemometrics and Intelligent Laboratory Systems*, **45**, 199-214, (1999)

20. Ruppen, D., D. Bonvin, and D. W. T. Rippin, "Implementation of Adaptive Optimal Operation for a Semi-batch Reaction system", *Comput. Chem. Eng.*, **22**, 185-189 (1998)
21. Soroush, M. and C. Kravaris, "Nonlinear Control of Batch Polymerization Reactor: An Experimental Study", *AIChE J.*, **38**(9), 1429-1448 (1992)
22. Srinivasan, B., S. Palanki, and D. Bonvin, "Dynamic Optimization of Batch Processes: I. Characterization of the Nominal Solution", *Comput. Chem. Eng.*, **27**, 1-26 (2003)
23. Sylvestre, E. A., W. H. Lawton, M.S. Maggio, "Curve Resolution Using a Postulated Chemical Reaction", *Technometrics*, **16**, 353-368, (1974)
24. Terwiesch, P. and M. Agarwal, "On-line Correction of Pre-determined input Profile for Batch Reactors", *Comput. Chem. Eng.*, **18**, S433-S437 (1994).
25. Van Impe, J. F. and G. Bastin, "Optimal Adaptive Control of Fed-batch Fermentation processes", *Control Eng. Practice*, **3**(7), 939-954 (1995).
26. Walter, W., 'Handbook of Organic Chemistry, Prentice Hall Europe', UK, 1996
27. Wiederkehr, H., "Examples of Process Improvement in the Fine Chemicals Industry", *Chemical Engineering Science*, **43**, 1783-1791 (1988)
28. Workman Jr., J. J., "Interpretive Spectroscopy of Near-Infrared", *Applied Spectroscopy Review*, **31**, 251-320, (1996)
29. Zafiriou, E. and J. M. Zhu, "Optimal Control of Semi-batch processes in the presence of Modeling Error", *In American Control Conference*, pages 1644-1649, San Diego, CA (1990).



## Appendices

### Appendix A: Derivation of Model Equations

For a semi-batch reactor mass balance can be mathematically written as

$$\Rightarrow \dot{N}_{j_{in}} - \dot{N}_{j_{out}} + \int_V r_j dV = \frac{dN_j}{dt} \quad (\text{A.1})$$

Where

$N_j = \text{moles of specie } j$

As

$$N_j = C_j V \quad (\text{A.2})$$

$$\Rightarrow \frac{dN_j}{dt} = \frac{d(C_j V)}{dt} = V \frac{dC_j}{dt} + C_j \frac{dV}{dt} \quad (\text{A.3})$$

Assuming no spatial variations in the rate of reaction gives

$$\int_V r_j dV = r_j V \quad (\text{A.4})$$

Assuming that the only cause of volume change is the volume of reactant injected gives

$$V = V_o + F_{AA} t \quad (\text{A.5})$$

This implies that

$$\frac{dV}{dt} = F_{AA} \quad (\text{A.6})$$

Since nothing exits the reactor

$$\dot{N}_{j_{out}} = 0 \quad (\text{A.7})$$

Substituting (1.4), (1.5), and (1.6) in (1.1) gives

$$\dot{N}_{Jin} + r_j V = V \frac{dC_j}{dt} + C_j F_{AA} \quad (\text{A.8})$$

Therefore the differential equation for change of concentration with respect to time for all the species in the system can be given by

$$\frac{dC_j}{dt} = \frac{\dot{N}_{Jin}}{V} + r_j - \frac{C_j F_{AA}}{V} \quad (\text{A.9})$$

### *Acetic Anhydride Mass Balance*

AA is being consumed by both reactions Rxn1 and Rxn2 therefore

$$r_{AA} = (-r_1 - r_2) \quad (\text{A.10})$$

And is the only reactant being added to the reactor therefore

$$\dot{N}_{AA} = F_{AA} C_{AAin} \quad (\text{A.11})$$

Substituting (1.11) and (1.12) into (3.13) gives the model equation for AA

$$\frac{d}{dt} C_{AA} = \frac{C_{AAin} - C_{AA}}{V} F_{AA} - r_1 - r_2 \quad (\text{A.12})$$

### *Acetyl Salicylic Acid Mass Balance*

ASA is only being produced by reaction R.1 therefore

$$r_{ASA} = r_1 \quad (\text{A.13})$$

And is not being added to the reactor therefore

$$\dot{N}_{ASA} = 0 \quad (\text{A.14})$$

Substituting (1.13) and (1.14) in (3.13) gives the model equation for ASA

$$\frac{d}{dt} C_{ASA} = -\frac{C_{ASA}}{V} F_{AA} + r_1 \quad (\text{A.15})$$

### ***Acetic Acid Mass Balance***

HA is being produced by both reactions Rxn1 and Rxn2 therefore

$$r_{HA} = r_1 + 2r_2 \quad (\text{A.16})$$

And is not being added to the reactor therefore

$$\dot{N}_{HA} = 0 \quad (\text{A.17})$$

Substituting (1.13) and (1.14) in (3.13) gives the model equation for HA

(A.24)

$$\frac{d}{dt}C_{HA} = -\frac{C_{HA}}{V}F_{AA} + r_1 + 2r_2 \quad (\text{A.18})$$

### ***Salicylic Acid Mass Balance***

SA is being consumed only by reaction R1 therefore

$$r_{SA} = -r_1 \quad (\text{A.19})$$

And is not being added to the reactor therefore

$$\dot{N}_{SA} = 0 \quad (\text{A.20})$$

Substituting (1.19) and (1.20) in (3.13) gives the model equation for SA

$$\frac{d}{dt}C_{SA} = -\frac{C_{SA}}{V}F_{AA} - r_1 \quad (\text{A.21})$$

### ***Water Mass Balance***

W is being consumed by reaction R2 only therefore

$$r_W = -r_2 \quad (\text{A.22})$$

And is not being added to the reactor therefore

$$\dot{N}_W = 0 \quad (\text{A.23})$$

Substituting (1.22) and (1.22) in (3.13) gives the model equation for W

$$\frac{d}{dt}C_W = -\frac{C_W}{V}F_{AA} - r_2 \quad (\text{A.24})$$

## Appendix B: Temperature Dependence of The Kinetic Constants

According to the Arrhenius equation the rate constants at different temperatures can be given by

$$k_1 = Ae^{-E_a/RT_1}$$

$$k_2 = Ae^{-E_a/RT_2}$$

$$\Rightarrow k_2 = k_1 e^{-\frac{E_a}{R}\left(\frac{1}{T_1} - \frac{1}{T_2}\right)}$$

if  $\Delta T$  is small

$\left(\frac{1}{T_1} - \frac{1}{T_2}\right)$  will be very small

$\Rightarrow e^{-\frac{E_a}{R}\left(\frac{1}{T_1} - \frac{1}{T_2}\right)}$  will be close to 1

$$\Rightarrow k_2 \approx k_1$$

where

A  $\equiv$  frequency factor

$E_a$   $\equiv$  activation energy

R  $\equiv$  gas constant

T  $\equiv$  temperature

## **Appendix C: MATLAB Code**

This function "ObjectiveFunction" accepts a vector, and names it par which is used to assign values to the parameters (k1, k2, k3, k4, CSA0, CAAin and etc), and returns a value for the objective function "obj\_func". To run this function files containing flow profile and spectra must be in the same directory as the "OF\_model".

To optimize ObjectiveFunction, type [opar,obj]=fminsearch('ObjectiveFunction',par) in the command line, this will return "opar" which will contain the optimized parameter values and "obj" which will contain the minimized objective function value and "par", is the vector that contains the initial guesses, should be in the workspace to assign what parameters are to be optimized go to the "Optimization Parameters" section below set the parameters to be optimized equal to "par(some #)" "some #" needs to be in ascending order starting at "1 " (ONE) and never repeated.

ObjectiveFunction uses initial guesses for the model parameters and generates a concentration profile matrix by solving the model equations using Euler's method. The by using the CCR method it generates a spectra matrix and then determines the sum of squared difference between the experimental spectra and model generated spectra. "%" indicates comments.

```

1. function obj_func_value = ObjectiveFunction(par)

2. %----- Non-Negativity -----%

3. N = size(par);

4. %--- N will contain the number of parameters in the par vector-----%

5. for i = 1:(N(2));

6. if (par(i) < 0);

7. obj_func_value = nan;

8. return

9. end

10. i = i + 1;

11. end

12. %-----%

13. %-----Optimization Parameters-----%

14. k1f = par(1);

15. %----k1f is the forward rate constant for Reaction R1-----%

16. k1r = par(2);

17. %----k1r is the reverse rate constant for Reaction R1-----%

```

18.  $k_2 = \text{par}(3);$

19. %---- $k_2$  is the rate constant for Reaction R2-----%

20.  $CW_0 = \text{par}(4);$

21. %----  $CW_0$  is the initial concentration of Water in the Batch-----%

22.  $CAA_{in} = \text{par}(5);$

23. %----  $CAA_{in}$  is the concentration of AA being injected----%

24.  $CSA_0 = \text{par}(6);$

25. %----  $CSA_0$  is the initial concentration of SA----%

26. %-----Initialization-----%

27.  $CAA_0 = 0;$

28. %----  $CAA_0$  is the initial concentration of AA in the batch-----%

29.  $CHA_0 = 0;$

30. %----  $CHA_0$  is the initial concentration of HA in the batch-----%

31.  $CASA_0 = 0;$

32. %----  $CAAA_0$  is the initial concentration of ASA in the batch-----%

33.  $CSA_{initial} = CSA_0;$

34. %----  $CSA_{initial}$  is the initial concentration of SA in the batch-----%



35. CWinitial = CW0;

36. %---- CWinitial is the initial concentration of W in the batch-----%

37. CF\_flowrate = 1;

38. %---- CF\_flowrate is the flowrate of the injection-----%

39. V0 = 0.020;

40. %---- V0 is the initial volume of the batch -----%

41. Vinitial = V0;

42. %---- V0 is the initial volume of the batch -----%

43. t0 = 0;

44. %---- t0 is used as a counter -----%

45. counter = 1;

46. %---- counter a variable used to count the total number of main loop executions -----%

47. h = 0.1;

48. %---- h is the step size used by the Euler's method -----%

49. CASA0 = 0;

50. %---- CASA0 is the initial concentration of ASA -----%

51. StopTime = 300;

```

52. %---- StopTime is for using spectra only till this value ----%

53. %----- Loading Files -----%

54. load('flowrate_c.mat','-mat');

55. %---- The variable in this file should be named "FLOWRATE" ----%

56. %---- "FLOWRATE" should be a vector containing ones and zeros one representing

57. %---- pump running and zero representing pump not running ----%

58. load('Amodel_1cL.mat','-mat');

59. %---- the variable in this file should be named "Amodel" ----%

60. % "Amodel" should be the spectra matrix (intensity vs. time(count))

61. %-----%

62. %-----Main Loop-----%

63. %-----Generates Concentration Profile Matrix-----%

64. while t0 <= StopTime

65. %---- Storing concentration values in to matrices ----%

66. FAA = ((FLOWRATE(counter))/1000)*CF_flowrate;

67. AA_flowrate(counter) = FAA;

68. SA_conc(counter) = CSA0;

```

```

69. AA_conc(counter) = CAA0;

70. W_conc(counter) = CW0;

71. HA_conc(counter) = CHA0;

72. ASA_conc(counter) = CASA0;

73. VOLUME(counter) = V0;

74. TIME(counter) = t0;

75. %---- End storing ----%

76. %-----Euler's Method Loop-----%

77. for iter2 = 0 : 9;

78. r1 = k1f * CSA0 * CAA0 - k1r * CASA0 * CHA0;

79. V0 = V0 + h * FAA;

80. CSA = CSA0 + h * ( -r1 - ( CSA0 / V0 ) * FAA );

81. CAA = CAA0 + h * ( -r1 - k2 * CW0 * CAA0 + ( ( CAAin - CAA0 ) / V0 ) * FAA );

82. CW = CW0 + h * ( -k2 * CW0 * CAA0 - ( CW0 / V0 ) * FAA );

83. CHA = CHA0 + h * ( r1 + 2 * k2 * CW0 * CAA0 - ( CHA0 / V0 ) * FAA );

84. CASA = CASA0 + h * ( r1 - ( CASA0 / V0 ) * FAA );

```

```
85. %---- Updating values ----%
86. t0 = t0 + h;
87. CSA0 = CSA;
88. CAA0 = CAA;
89. CW0 = CW;
90. CHA0 = CHA;
91. CASA0 = CASA;
92. %---- Updating values ends----%
93. if t0 > StopTime;
94. break
95. end
96. iter2 = iter2 + 1;
97. end
98. %-----Euler's Method Loop Ends-----%
99. counter = counter + 1;
100. if counter > StopTime
101. break
```

```

102. end

103. %-----Main Loop Ends-----%

104. end

105. %---- Storing the concentration of the species that absorb UV/Vis ----%

106. conc_model(:,1)=SA_conc(:);

107. conc_model(:,2)=ASA_conc(:);

108. %---- End storing ----%

109. A = (sp(1:StopTime,:));

110. C = conc_model(1:StopTime,:);

111. %---- The CCR method ----%

112. e = A - C * ( C \ A);

113. ee = e.*e;

114. %-----dyadic multiplication-----%

115. E = C\A;

116. Anew = C*E;

117. %---- CCR method ends ----%

118. obj_func_value = sum(sum(ee))

```

```

119. %---- Calculating volume and time required to reach endpoint ----%

120. VOLUME = VOLUME * 1000;

121. Vinitial = Vinitial * 1000;

122. Vadded = (VOLUME(end) - Vinitial);

123. AA_molesreq = CSAinitial * Vinitial + CWinitial * Vinitial - Vadded * CAAin;

124. Vreq = AA_molesreq/CAAin

125. CAAstar = AA_molesreq / (VOLUME(end) + Vreq);

126. CSAstar = SA_conc(end) / (VOLUME(end) + Vreq);

127. a = CAAstar - CSAstar;

128. SAtol = 0.001;

129. trxn = (quad(@intgfun,SAtol,CSAstar,[],[],a))/k1f;

130. %---- Calculating time required to reach endpoint ----%

131. tdel = Vreq / (CF_flowrate*10);

132. treq = tdel + trxn

133. function F = intgfun(x,a)

134. %---- Function used to find time required to reach endpoint ----%

135. F = 1./((x.^2 + a.*x));

```

136. return

137. %-----End of Program-----%

## **Appendix D: Using “fminsearch”**

This section has been adapted from MATLAB (version 6.5.0.180913a Release 13) help documentation.

Minimizes a function of several variables

### ***Syntax***

`x = fminsearch(fun,x0)`

`x = fminsearch(fun,x0,options)`

`x = fminsearch(fun,x0,options,P1,P2,...)`

`[x,fval] = fminsearch(...)`

`[x,fval,exitflag] = fminsearch(...)`

`[x,fval,exitflag,output] = fminsearch(...)`

### ***Description***

`fminsearch` finds the minimum of a scalar function of several variables, starting at an initial estimate. This is generally referred to as unconstrained nonlinear optimization.

`x = fminsearch(fun,x0)` starts at the point `x0` and finds a local minimum `x` of the function described in `fun`. `x0` can be a scalar, vector, or matrix.

`x = fminsearch(fun,x0,options)` minimizes with the optimization parameters specified in the structure `options`. You can define these parameters using the `optimset` function.

`fminsearch` uses these `options` structure fields:

**Display**      Level of display. 'off' displays no output; 'iter' displays output at each iteration; 'final' displays just the final output; 'notify' (default) displays output only if the function does not converge.



**MaxFunEvals** Maximum number of function evaluations allowed

**MaxIter** Maximum number of iterations allowed.

**TolX** Termination tolerance on  $x$ .

**TolFun** Termination tolerance on the function value.

$x = \text{fminsearch}(\text{fun}, x_0, \text{options}, P_1, P_2, \dots)$  passes the problem-dependent parameters  $P_1$ ,  $P_2$ , etc., directly to the function  $\text{fun}$ . Use  $\text{options} = []$  as a placeholder if no options are set.

$[x, \text{fval}] = \text{fminsearch}(\dots)$  returns in  $\text{fval}$  the value of the objective function  $\text{fun}$  at the solution  $x$ .

$[x, \text{fval}, \text{exitflag}] = \text{fminsearch}(\dots)$  returns a value  $\text{exitflag}$  that describes the exit condition of  $\text{fminsearch}$ :

$>0$  Indicates that the function converged to a solution  $x$ .

$0$  Indicates that the maximum number of function evaluations was exceeded.

$<0$  Indicates that the function did not converge to a solution.

$[x, \text{fval}, \text{exitflag}, \text{output}] = \text{fminsearch}(\dots)$  returns a structure  $\text{output}$  that contains information about the optimization:

$\text{output.algorithm}$  The algorithm used  
 $\text{output.funcCount}$  The number of function evaluations

$\text{output.iterations}$  The number of iterations taken

### ***Arguments***

$\text{fun}$  is the function to be minimized. It accepts an input  $x$  and returns a scalar  $f$ , the objective function evaluated at  $x$ . The function  $\text{fun}$  can be specified as a function handle.

$x = \text{fminsearch}(@\text{myfun}, x_0, A, b)$

where  $\text{myfun}$  is a MATLAB function such as  $\text{function } f = \text{myfun}(x)$

```
f = ...      % Compute function value at x
```

fun can also be an inline object.

```
x = fminsearch(inline('sin(x*x)'),x0,A,b);
```

Other arguments are described in the syntax descriptions above.

### **Examples**

A classic test example for multidimensional minimization is the Rosenbrock banana function

$$f(x) = 100(x_2 - x_1^2)^2 + (1 - x_1)^2$$

The minimum is at (1,1) and has the value 0. The traditional starting point is (-1.2,1). The

M-file banana.m defines the function. function f = banana(x)

```
f = 100*(x(2)-x(1)^2)^2+(1-x(1))^2;
```

The statement

```
[x,fval] = fminsearch(@banana,[-1.2, 1])
```

produces

```
x =
```

```
1.0000  1.0000
```

```
fval =
```

```
8.1777e-010
```

This indicates that the minimizer was found to at least four decimal places with a value near zero. Move the location of the minimum to the point [a,a<sup>2</sup>] by adding a second parameter to banana.m.

```
function f = banana(x,a)
```

```
if nargin < 2, a = 1; end
```

```
f = 100*(x(2)-x(1)^2)^2+(a-x(1))^2;
```

Then the statement

```
[x,fval] = fminsearch(@banana, [-1.2, 1], optimset('TolX',1e-8), sqrt(2));
```

sets the new parameter to `sqrt(2)` and seeks the minimum to an accuracy higher than the default on `x`.

### ***Algorithm***

`fminsearch` uses the simplex search method of Lagarias, *et al.* 1998. This is a direct search method that does not use numerical or analytic gradients. If `n` is the length of `x`, a simplex in `n`-dimensional space is characterized by the `n+1` distinct vectors that are its vertices. In two-space, a simplex is a triangle; in three-space, it is a pyramid. At each step of the search, a new point in or near the current simplex is generated. The function value at the new point is compared with the function's values at the vertices of the simplex and, usually, one of the vertices is replaced by the new point, giving a new simplex. This step is repeated until the diameter of the simplex is less than the specified tolerance.

### ***Limitations***

fminsearch can often handle discontinuity, particularly if it does not occur near the solution. fminsearch may only give local solutions. fminsearch only minimizes over the real numbers, that is,  $x$  must only consist of real numbers and  $f(x)$  must only return real numbers. When  $x$  has complex variables, they must be split into real and imaginary parts.

VITA



Syed Samir Alam

Candidate for the Degree of

Master of Science

Thesis: Monitoring and Characterization of a Batch Reaction – for on-line recipe adjustment

Major Field: Chemical Engineering

Biographical:

Personal Data: Born in Hail, Saudi Arabia, April 19, 1978.

Education:

Received Bachelor of Science in Chemical Engineering from Oklahoma State University, Stillwater, OK, in May 2001. Completed the requirements for Master of Science degree in Chemical Engineering from Oklahoma State University in December 2003.

Professional Experience:

Graduate Assistant, Oklahoma State University, Stillwater, OK (2001-2003);